Climate change threatens archeologically significant ice patches: insights into their age, internal structure, mass balance and climate sensitivity

Rune Strand Ødegård[1] , Atle Nesje[2] , Ketil Isaksen[3],
Liss Marie Andreassen[4], Trond Eiken[5] , Margit Schwikowski[6]
and Chiara Uglietti[6]

[1]{Norwegian University of Science and Technology, Gjøvik, Norway}

[2]{University of Bergen, Bergen, Norway}

[3]{Norwegian Meteorological Institute, Oslo, Norway}

[4]{Norwegian Water Resources and Energy Directorate, Oslo, Norway}

[5]{Department of Geosciences, University of Oslo, Oslo, Norway}

[6]{Paul Scherrer Institute, Villigen, Switzerland}

Correspondence to: R.S. Ødegård (rune.oedegaard@ntnu.no)

Abstract

Despite numerous spectacular archaeological discoveries worldwide related to melting ice patches and the emerging field of glacial archaeology, governing processes related to ice patch development during Holocene and their sensitivity to climate change are still largely unexplored. Here we present new results from an extensive 6-year (2009-2015) field experiment at Juvfonne ice patch in Jotunheimen in central southern Norway. Our results show that the ice patch existed continuously since the late Mesolithic period. Organic-rich layers and carbonaceous aerosols embedded in clear ice shows ages spanning from modern at the surface to ca. ~~6200 BCE~~7600 cal. years BP at the bottom. This is the oldest dating of ice in mainland Norway. ~~Moss mats appearing along the margin of Juvfonne in 2014 were covered by the expanding ice patch~~The expanding ice patch covered moss mats appearing along the margin of Juvfonne in 2014 about 2000 years ago. During the study ~~period~~period, the mass balance record shows a strong negative balance, and the net balance is highly

asymmetric over short distances. Snow accumulation is poorly correlated with winter precipitation and single storm events may contribute significantly to the total winter balance. Snow accumulation is approx. 20 % higher in the frontal area compared to the upper central part of the ice patch. The thermal regime in Juvfonne is similar to what is found close to the equilibrium line of nearby glaciers. There is sufficient melt water to bring the permeable snowpack to an isothermal state within a few weeks in early summer. Below the seasonal snowpack ~~ice~~ice, temperatures are between -2 and -4°C, similar to the surrounding permafrost terrain. Juvfonne has clear ice stratification of isochronic origin. The cumulative deformation of ice over millennia could explain the observed curved layering in the basal parts of the ice patch, which makes it difficult to relate the present thickness to previous thickness of the ice patch. Ice deformation and surface processes (i.e. wind and melt water) may have caused significant displacement of artefacts from their original position. ~~Thus~~Thus, the dating and position of artefacts cannot be used directly to reconstruct previous ice patch extent. In the perspective of surface energy and mass ~~balance;~~balance, ice patches are in the transition zone between permafrost terrain and glaciers. Future research will need to carefully address this interaction to build reliable models.

1 Introduction

The emergence of glacial archaeology is described by Andrews and Mackay (2012) and Dixon et al. (2014). In archaeology, the term ‘glacial archaeology’ or ‘snow patch archaeology’ refers to several alpine contexts in different regions of the world (Callanan, 2010). The release of Ötzi’s 5300 year old body from the ice in northern Italy marked the beginning of a number of remarkable archaeological discoveries world-wide connected to melting ice and thawing permafrost in the high mountains (Spindler, 1994). Discoveries are known from the Alps (Grosjean et al., 2007; Suter et al., 2005), mummies in Greenland (Hansen et al., 1985) and the Andes Mountains (Ceruti, 2004), and from archaeological finds at retreating ice patches in North America (Brunswig, 2014; Dixon et al., 2005; Farnell et al., 2004; Hare et al., 2012; Lee, 2012; Meulendyk et al., 2012). When analysing the number of artefacts on a global scale during the Holocene, there is a negative correlation between periods of glacial advance and the number of artefacts. This is particularly the case in the Alps and North America (Reckin, 2013), but a similar pattern is also found in Norway (Nesje et al., 2012). The question is if this is caused by changes in climate dependent preservation conditions or decreased human use of these areas in periods of cold climate.

In Norway, there has been an increasing focus on ice patches since the extreme melting in southern Norway in the autumn of 2006. There are about 3000 known artefact finds globally from ice patches. Most of these have melted out during the last three decades. Approximately 2000 of these archaeological finds are in central southern Norway, making it by far the most find-rich region in the world (Curry, 2014, pers.comm. Lars Pilø).

Among the most spectacular finds is a Bronze Age leather shoe that melted out in late autumn 2006 and a well-preserved tunic dated between 230-390 (Common Era) CE (Finstad and Vedeler, 2008; Vedeler and Jørgensen, 2013). The shoe was dated to be around 3400 years old (1429-1257 Before Common Era (BCE)), and is by far the oldest shoe found in Norway. Dates are given in calibrated ages (BCE/CE) including 1 sigma errors (σ) when referencing archaeological finds. Radiocarbon dates from ice patches are referenced as calibrated years Before Present (BP=1950CE) including 1 sigma errors (σ).~~.~~

The geoscience of old ice patches is still in its infancy and the geoscience literature about ice patches is sparse compared to glacial archaeology. Within the glaciological community it is commonly differentiated~~d~~ between glaciers and snowfields and active or inactive ice (UNESCO, 1970). Snowfields may be seasonal or perennial. Seasonal snowfields melt during the summer. Perennial snowfields exist for two years or more. Smaller ice bodies without significant movement may be remnants of a past active glacier or a perennial snowfield and are commonly referred to as glacierets. In this paper, we use ice patch for perennial snowfields and glacierets. Ice patches are, in contrast to glaciers, mostly stagnant and therefore, do not convey mass from an accumulation towards an ablation area. In fact, ice patches often do not exhibit distinct glacier facies such as a firn area. In the wet-snow zone, the transformation of snow to ice is fast by metamorphism and refreezing of melt water. (Kawasaki et al., 1993). Ice patches and surrounding terrain are generally underlain by permafrost (Haeberli et al., 2004). There are few studies related to the thermal regime, mass balance and dynamics (Eveland et al., 2013; Fukui, 2003; Fukui and Iida, 2011; Sato et al., 1984). Fujita et al. (2010) concluded that they exist below the altitude of the regional equilibrium-line altitude (ELA) of glaciers. A study by Glazirin et al. (2004) showed that they can modify the nearby wind field. The mentioned studies have documented feedbacks between ice patch size and both summer ablation and winter snow accumulation. The spatial variability of the turbulent fluxes in an alpine terrain is of particular interest to ice patches. Ice patches are influenced by advective heat transfer in summer (Essery et al., 2006; Mott et al., 2015; Pohl et al., 2006). The sensible heat flux is reported to be to twice the net radiation input for melting snow (Morris, 1989).

Despite some progress in these studies, the state of knowledge is not at a level to design reliable models of how ice patches have developed during the Holocene and to evaluate their sensitivity to future climate changes. The main objective of this study is to help fill this knowledge gap~~.~~ based on a 6-year field experiment at Juvfonne ice patch, located in Jotunheimen in central southern Norway (Fig. 1 and 2, 61.676ºN, 8.354ºE).

The overall objective of this study is to do an exploratory data analysis of field data to better understand the governing processes of ice patch mass balance and Holocene development. The long-term objective is to design reliable models of the growth and decline of ice patches in this alpine environment. One additional dimension in this research is the cooperation with the archaeologist to help them in their interpretation of finds and give them some advice regarding future development. A multi-disciplinary approach was chosen, combining a set of new geophysical data, radiocarbon dating, mass balance measurements and visual observations from two 30-70 m tunnels that were~~as~~ excavated into the central parts of the ice patch in order to better understand (1) the age, (2) the mass balance, (3) the thermal regime, (4) ice layering and deformation on Holocene time scale and finally (5) the physical processes relevant to artefact displacement and preservation.

Formatted: English (United Kingdom)

2 Field site and physical setting

~~The presented research is based on a 6-year field experiment at Juvfonne ice patch, located in Jotunheimen in central southern Norway (Fig. 1 and 2, 61.676ºN, 8.354ºE).~~ In ~~this area~~central southern Norway the archaeologists have so far identified more than 65 sites with finds related to ice patches, but many sites with potential finds have not been checked in the field. The archaeological finds are related to reindeer hunting. The snowfields are an important refuge for the reindeers during hot summer days, giving them relief from pestering insects. The focus of this study is the ice patch Juvfonne and the surrounding terrain (Fig. 1 and 2). This site is a well-preserved Iron Age hunting 'station' documented by more than 600 registered wooden artefacts and 50 hunting blinds. Radiocarbon dating of artefacts shows ages in two separate time intervals, 246-534 CE and 804-898 CE (Nesje et al., 2012). The geoscience studies at Juvfonne started in 2009 (Ødegård et al., 2011). Nesje et al. (2012) gave a comprehensive presentation and discussion of archaeological finds in central southern Norway related to Late Holocene climate history.

The width of the ice patch is approx. 500 m and upslope length 350 m. Juvfonne had an area of 0.15 km^2 and ranged in altitude from 1839 to 1993 m a.s.l. in 2010 (Andreassen, 2011). The mean surface slope is 17 degrees and the ice patch has a ~~north-easterly~~north easterly aspect.

Due to snowdrift by prevailing westerly winds during the accumulation season, Juvfonne is below the regional temperature-precipitation equilibrium-line altitude (TP-ELA). Annual surface mass balance measurements have been conducted on three glaciers (since 1949 at Storbreen and 1962 at Hellstugubreen and Gråsubreen) in the Jotunheimen mountain region (Andreassen et al., 2005; Andreassen and Winswold, 2012). The ELA increases with distance from coast from 1780 m a.s.l. at Storbreen to 2150 m a.s.l. at Gråsubreen (Kjøllmoen et al., 2011). Except for a transient mass surplus from 1989-1995 due to increased winter precipitation in this period, the glaciers have lost mass. Map surveys and inventory data show a reduction in area of the glaciers in Jotunheimen of about 10 % from the 1960s to 2003 (Andreassen et al., 2008).

Juvfonne is well within the mountain permafrost zone. Present permafrost thicknesses at elevations where we find perennial ice patches (~> 1700 m a.s.l.) can be estimated to be more than 100 m. Observations of ground thermal regimes (Farbrot et al., 2011; Harris et al., 2009), bottom temperature of snow cover (BTS) (Farbrot et al., 2011; Isaksen et al., 2002; Ødegård, 1993) and geophysical surveys to delineate the altitudinal limit of the permafrost (Hauck et al., 2004; Isaksen et al., 2011) along with spatial numerical equilibrium and transient permafrost models (Gisnås et al., 2013; Gisnås et al., 2015; Hipp et al., 2012; Westermann et al., 2013) indicate a lower limit of permafrost at 1450-1600 m a.s.l. in the area.

Juvfonne is at a distance of 750 m and at the same altitude as the permafrost boreholes (the P30 and 31 Permafrost and Climate in Europe (PACE) boreholes) and climate monitoring site at Juvvasshøe (Sollid et al., 2000)(see Fig. 2). The site has a record of ground temperatures and meteorological observations since September 1999. Mean annual air temperature for the period 2000-2015 is –3.5 °C. At 15 m depth, the permafrost temperature ranges from a minimum of -3.1 °C in 1999 to a maximum of -2.5°C recorded in 2008. The active layer thickness has varied between 2.0 and 2.4 m and permafrost thickness is estimated to exceed

Formatted: Font: (Default) Times New Roman, 12 pt, Font color: Auto, English (United Kingdom)

Formatted: Font: (Default) Times New Roman, 12 pt, Font color: Auto, English (United Kingdom)

Formatted: Font: (Default) Times New Roman, 12 pt, Font color: Auto, English (United Kingdom)

Formatted: Font: (Default) Times New Roman, 12 pt, Font color: Auto, English (United Kingdom)

Formatted: Font: (Default) Times New Roman, 12 pt, Font color: Auto, English (United Kingdom)

300 m (Isaksen et al., 2011). In ~~2008~~2008, an altitudinal transect of ~~permafrost~~ boreholes and adjacent air temperature ~~measurements~~ sensors were installed ~~in the area~~at three sites ranging from shallow seasonal frost to permafrost (Farbrot et al 2013).

For the period ~~1961-1990~~1961-1990, the mean annual precipitation is estimated to be between 800mm a^{-1} and 1000mm a^{-1} at 1900 m a.s.l. (Norwegian Meteorological Institute, unpublished data).

Results of analysis from sediment cores in the nearby Juvvatnet was used to reconstruct the glacier activity of Kjelebrea and Vesljuvbrea (Nesje et al., 2012) following the methodology described by Bakke et al. (2010). The results indicate that the late Holocene variations of these glaciers are largely in agreement with size variations of other glaciers in the Jotunheimen area (Matthews and Dresser, 2008; Nesje, 2009). Lichenometry suggests that the margin of Juvfonne extended ~250 m from its present position during the 'Little Ice Age"(LIA) maximum extent in the mid-18th century (Nesje et al., 2012).

3 Methods

3.1 Georadar

The ice patch was surveyed by a RAMAC georadar 23 September 2009 and 1 March 2012, using a high frequency antenna of 250~~500~~ MHz. The dielectric constant of ice was set to be 3.2, giving a phase velocity of 168 m μs^{-1}. ~~—~~Georadar data and positioning data from the Global Navigation Satellite System (GNSS) were manually digitized to obtain a point dataset of ice thickness and bed topography. The point datasets were interpolated to get an ice thickness map and a digital terrain model (DTM) of the ice patch bed. Obvious artefacts caused by the interpolation technique were manually removed. ~~Totally~~ A total of 40 independent control points gave an estimated standard deviation of 1.1 m, and a maximum error of 2.6 m. The control points were obtained by point measurements (GNSS) in the recently exposed area.

3.2 Laser scanning

The ice patch and surrounding terrain was scanned with an air-borne laser (Leica ALS70) on 17 September 2011. The company COWI AS, on assignment from Norwegian Water

Formatted: English (United States)

Resources and Energy Directorate, carried out the laser scanning and the processing of the data. The flight altitude was 10100-11800 feet (3078-3597 m a.s.l.). The area was scanned with 5 points m^2. Quality controls and accuracy assessments revealed accuracy better than 0.1 m in surface elevation. Aerial photos were taken on the same day. These data were used to produce a high quality DTM and orthophotos of the ice patch surface and surrounding terrain. The DTM was resampled to a resolution of 1 m.

~~The ice patch and surrounding terrain was scanned with an air-borne laser on 17 September 2011. The area was scanned with 5 points m-2 with accuracy better than 0.1 m. Aerial photos were taken on the same day. These data were used to produce a high quality DTM and orthophotos of the ice patch surface and surrounding terrain. The DTM was resampled to a resolution of 1 m.~~

3.3 Mass balance and front measurements

S~~Standard s~~urface mass balance measurements of winter accumulation (snow depth at 20-60 sites and density at 1 site) and ablation (at 1-4 stakes) were made following standard methods for the melting seasons of 2010-2015 (Andreassen, 2011). Distance to the terminus ~~has been~~was measured from two points outside the ice patch (Fig. 3a) in August or early September using a laser distance meter.

The extent of the Juvfonne ice patch was surveyed by foot with GNSS with a Topcon receiver mounted on a ~~back pack~~backpack and one reference receiver mounted in a fixed base point (Fig. 3a, Table 1). The GNSS data was processed with Topcon software TTOOLS version 8.

~~The extent of the Juvfonne ice patch has been surveyed by foot with differential GNSS mounted on a back pack (Fig 3a, Table 1).~~ Surveys ~~have been~~were done annually in August or September from 2010 to 2015, but the survey from 2012 was only done along the lower part due to snow conditions. Areal extent was also determined by digitising outlines from orthophotos from 2011 and from topographical maps from the Norwegian mapping authorities in 1981 and 2004. Furthermore, outlines from Landsat inventories from 1997 and 2003 were used (Andreassen et al., 2008; Winsvold et al., 2014). The accuracy of the differential GNSS are within 1m, the accuracy of the N50 within 5 m and the accuracy of the Landsat mapping within 30 m. The standard deviation in height of the GNSS measurements is on the range 10-20 cm giving ±2 standard deviations of 0.6 m.

Formatted: Not Superscript/ Subscript

Formatted: No underline

Formatted: Font: (Default) Times New Roman, 12 pt, Font color: Black, English (United Kingdom)

Formatted: Justified, Space Before: 6 pt, Line spacing: 1,5 lines, Adjust space between Latin and Asian text, Adjust space between Asian text and numbers

Formatted: Font: (Default) Times New Roman, 12 pt, Font color: Black, English (United Kingdom)

Formatted: Font: (Default) Times New Roman, 12 pt, Font color: Black, English (United Kingdom)

Formatted: Font: (Default) Times New Roman, 12 pt, Font color: Black, English (United Kingdom)

Formatted: Font: (Default) Times New Roman, 12 pt, Font color: Black, English (United Kingdom)

3.4 Meteorological measurements

Hourly meteorological data was obtained from the automatic weather station (AWS) at Juvvasshøe (1894 m a.s.l.). It is the highest official meteorological station in Norway, and is freely exposed and representative for this study, except for wind speed.~~It is the highest official meteorological station in Norway and is freely exposed and highly representative for this study.~~ The first station was set up in 1999 (Isaksen et al., 2003) and a new official weather station was established at the same site in June 2009. One additional station recording hourly snow depth was set up in autumn 2011 in front of Juvfonne (95 m from the eastern margin of the snowfield). Hourly data on snow depth is scarce in the high mountains in Scandinavia. Observed air temperature and wind speed on Juvvasshøe were compared against the 1971-2000 climatological normal based on interpolated air temperature data from seNorge (Engeset et al., 2004) and daily observations of wind speed from Fokstugu (973 m a.s.l.), 70 km NE of Juvasshøe, which was the best nearby correlated meteorological station having long-time series.

A thermistor cable was installed in a 10 m deep borehole in 2009 to record ice temperatures. Temperatures were recorded every 3 hours until late September 2011 with an accuracy of 0.05 ºC (1 standard deviation). The entire thermistor cable melted out in September 2014.~~).~~ Additional thermistor measurements were made in the snow and ice at the onset of thaw in spring 2010.

3.5 Radiocarbon dating

In May 2010, a 30 m long ice tunnel was excavated in the Juvfonne ice patch. During spring ~~2012~~2012, a new 70 m~~etre~~ long tunnel was excavated into the central parts of the ice patch. The tunnels were excavated with specially designed ice axes causing minimal disturbance to the surrounding ice. The tunnels gave an excellent opportunity to verify the radar data and to collect organic ~~material~~ material and ice for ~~for Accelerator Mass Spectrometry (AMS)~~ radiocarbon dating. Dateable organic material is available, but there are no continuous layers of organic material. Radiocarbons dating prior to 2012 are published in (Nesje et al., 2012; Zapf et al., 2013; Ødegård et al., 2011). Conventional ^{14}C ages were calibrated using OxCal v4.2.4 software (Bronk Ramsey and Lee, 2013) with the IntCal13 calibration curve (Reimer et al., 2013).

Formatted: Font: Not Italic, Font color: Black, English (United States)

Formatted: Font: Not Italic, Font color: Black, English (United States)

The organic debris has been collected from the walls and below the floor of the ice tunnels (5 samples from the tunnel excavated in 2010 and 5 samples from the tunnel excavated in 2012 – Table 2) and organic debris melting out at the front of which two datings are reported in this paper. Nine additional datings were published by Nesje et al. (2012).

The recently developed method for radiocarbon dating of ice utilizes the organic carbon fraction of carbonaceous aerosols scavenged from the atmosphere during snowfall and embedded into the ice matrix (Jenk et al., 2009; Sigl et al., 2009). This method was tested with 11 samples from Juvfonne in 2011 by comparing for the first time ^{14}C ages determined from carbonaceous particles with ^{14}C ages conventionally obtained from organic remains found in the ice (Zapf et al., 2013). The 2011 samples are JUV1 and JUV2 adjacent to the dated organic-rich layers in the 2010 tunnel and a surface sample JUV3 (Table 2). In summer 2015 five samples of clear ice were collected adjacent to the plant fragment layer located just above the bed in the tunnel excavated in 2012 (JUV0, Table 2 ~~and 3~~). All blocks of ice (~20 × 15 × 10 cm) were extracted with a pre-cleaned chainsaw and were subsequently divided into smaller pieces. All ice blocks were transported frozen to Paul Scherrer Institute (PSI, Switzerland), decontaminated in a cold room by removing the outer layer (0.3 mm) with a pre cleaned stainless steel band saw and by rinsing the ice samples with ultra-pure water in a class 100 clean room (Jenk et al., 2007).

Insoluble carbonaceous particles are filtered onto preheated quartz fibre filters (Pallflex Tissuquartz, 2500QAO-UP) and combusted with a thermo-optical organic carbon/elemental carbon (OC/EC) analyser (Model4L, Sunset Laboratory Inc., USA), using a well-established protocol (Swiss_4S) for OC/EC separation (Zhang et al., 2012). Analyses of ^{14}C were conducted using the 200 kV compact radiocarbon system ‘MICADAS’ at the University of Bern (LARA laboratory), equipped with a gas ion source coupled to the Sunset instrument, allowing measuring ^{14}C directly in CO_2 of 3-100 µg C with an uncertainty level as low as 1% (Ruff et al., 2010).

Dates are given in calibrated ages ~~(BCE/CE)~~BP (BP=1950 CE) including 1 sigma errors (σ).

4 Results

4.1 Ice thickness and ice layering

The bed reflection was clearly seen in the radar plots (see example in Fig. 4). In addition the ice layering was detected on most of the plots, probably due to density differences in the ice layers (air bubbles) (Hamran et al., 2009) or organic layers. Georadar soundings from 2009 revealed a maximum ice thickness of 17-19 m (Ødegård et al., 2011). The near-surface reflection horizons are nearly parallel to the present surface. At depth, curved reflection horizons are observed. In the ice tunnels the curved layers can be directly observed forming a distinct angular discontinuity with the surface-parallel ice layers (Fig. 5). The surface parallel layers have melted away since 2009 in the central and southern parts of the ice patch (Fig 6). The DTM obtained from laser scanning combined with the bottom topography from the georadar gave a volume of 710,000 m^3 in late August 2011 (mean thickness 5.6 m). The surface of Juvfonne in September 2011 was used as the reference surface for the depth map (Fig. 3b). The maximum depth was 16 m close to thethe inner part of ice tunnel excavated in 2012. In this area the surface slope is about 18 degrees.

4.2 Mass balance, front changes and areal extent

Only one of the mass balance stakes (J2) existed continuously from autumn 2009 to spring 2015 (Figs. 7 and 8). Stake J2 is in the central part of the ice patch (Fig. 3a).

Snow sounding measurements (N=232) range from 0.6-4.8 m over the period 2010-2015. Mean snow depth is 2.6 m (1.2 m w.e.). Some years show a pattern where most snow accumulates on the leeward side of the prevailing wind the previous winter, but this is not consistent. Inter annual variation accounts for 66%. The accumulation was further investigated by analysing the deviation from mean each year. This dataset contains a significant trend with increased accumulation towards the front (Fig. 3c and Table 4). The difference between the upper central area and the front is 0.2 m w.e (Fig. 3c), which corresponds to approx. 20% increase in accumulation.

The total mass loss is measured to 10 m of ice at the site of the thermistor measurements (Fig. 3a). The 10-metre thermistor cable installed on the 29th of October 2009 melted out in mid-September 2014. The total mass loss at stake J2 was 10.5 m w.e. during the same period.

Elevation changes from September 2011 to September 2014 are shown in Fig. 3d. These results are based on the laser scanning in 2011 and differential GNSS-tracking in 2014. The measurements show a highly significant asymmetric pattern with close to zero surface elevation changes in the western part and surface lowering of 3-5 m in the eastern and central part of the ice patch. This strong gradient is measured over a distance of just 200 m at approximately the same altitude. The part with most negative change has more than average accumulation.

Front change measurements ~~were initiated~~started in 2009 at JF1 and in 2010 at JF2 (Fig. 9). The measurements revealed that Juvfonne retreated in all years except in 2012 and 2015 where the ice patch increased its size due to excessive snow that formed a thin ice and snow layer around the margin. The total retreat 2009-2014 is -52 m measured from JF1 and over 2010-2014 the mean change is 44 m (-51m from JF1 and -38 m from JF2).

The annual extent measurements (2010-2015) show area fluctuations of the margin, varying from 0.101 km^2 (9 September 2014) to a maximum of 0.186 km^2 on 11 September 2015 (Table 1). The extent measurements show that the ice patch shrinks and grows along the whole margin. Furthermore, observations in field show that the ice is very thin along the margins. In 2015, seasonal snow covered the entire margin, and the measured area of 0.186 km^2 is thus only to be considered a maximum extent, not the actual ice patch area.

Formatted: Superscript

4.3 Climate parameters

Air temperature and wind speed at Juvvasshøe for the period 2000-2015 are outlined in Fig. 10 a-b over the ablation season (June-September). The mean June-September air temperature in this period is 3.2 °C (1.0 °C above the 1971-2000 mean). Air temperatures, near-ground surface temperatures and frequency of days with daily mean air temperature above 0 °C (the two latter are not shown in Fig. 10) are high in summers 2002, 2003, 2006, 2011 and 2014, and especially 2006. Observations from nearby weather stations with long climate series reported record-breaking temperatures in late summer and autumn 2006. In the investigation period 2009-2015 the coldest summer was 2012, which was the only summer below the 1971-2000 mean (Fig. 10).

Due to the sheltered setting of Juvfonne compared to the meteorological stations, strong breeze (wind speed above 10.8 ms-1) was used as a lower limit to get sufficient high wind speeds for effective and enhanced turbulent fluxes at Juvfonne. In general there is a high

Formatted: Font: Not Italic, Font color: Black, English (United Kingdom) frequency (35-58 days per season) of strong breeze during the period 2009-2015 (Fig. 10b). ~~In general there is a high frequency (35-58 days per season) of strong breeze during the period 2009-2015 (Fig. 10b).~~ Comparing wind data from the AWS at Fokstugu indicates two to three times more frequent strong wind than 1971-2000 mean during the investigation period. Observed incoming short- and longwave radiation from Juvvasshøe (not shown) show no clear patterns related to single summers, but 2011 ~~peaks~~ stands out as the summer with greatest incoming ~~longwave~~long wave radiation.

For snow accumulation or abrasion on ice patches wind speed and wind direction is crucial (Dadic et al., 2010; Lehning et al., 2008). There are great variations from year to year in respect to frequency of strong gale and wind direction. During the two stormiest winters 2011-12 and 2013-14, the frequency of strong gale was 15.7 % and 17.3 %, respectively (Fig. 11).~~For snow accumulation or abrasion on ice patches wind speed and wind direction is crucial. Results reveal (not shown here) that strong wind is frequent during winter. There are great variations from year to year and between early and late winter in respect to frequency of strong gale and wind direction.~~

Formatted: Font: Not Italic, Font color: Black, English (United States)

Formatted: Font: Not Italic, Font color: Black, English (United States)

Formatted: Font: Not Italic, Font color: Black, English (United States)

4.4 Snow measurements and modelling

The automatic snow depth observations in front of Juvfonne show great hourly to daily variability and there is distinct different pattern of snow accumulation between the four winter seasons (Fig. 12~~1~~). The greatest increase in snow depth during early and mid-winter in all years is related to storm events. This is also the case for strong snow depth decrease events (mainly due to ~~abrasion~~wind scouring). Comparing the observed and modeled snow depths (which don't~~not~~ take into account redistribution of snow by wind), it is clear that much of the accumulation is not correlated with precipitation (Fig. 12~~1~~). The modelled snow depth for Juvfonne was obtained from a precipitation/degree-day model operating on 1×1 km^2 developed for a web-based system (http://senorge.no/) for producing daily snow maps for Norway (Engeset et al., 2004; Saloranto, 2012). A similar poor correlation (r^2=0.24) is also found for very small glaciers in the Alps (Huss and Fischer, 2016)

The observed melt in central parts (J2) was compared with a degree-day model using typical values calculated from nearby glaciers (Fig. 7a) (Laumann and Reeh, 1993). This modelling shows a quite good fit except the 2010 season. In this ~~season~~season, the summer balance was about twice the outcome of the degree-day model.

4.5 Temperature of ice and permafrost

Temperature measurements in Juvfonne reveal 10-m depth ice temperature in the range of -2 to -4 ºC (Fig. 13~~2~~). The ice and snow temperature results show that the Juvfonne ice patch is cold-based and underlain by permafrost~~ (Fig. 13)~~. The measurements at 5-10 m depth in the ice are similar to the measurements in the nearby permafrost borehole at Juvvasshøe (Fig. 13~~2~~). In spring, the melt water percolates and refreezes in the snowpack until the snow is isothermal at a temperature close to 0ºC (Fig. 14). There is cold ice below the level of meltwater percolation, which means that there is a heat flow into the ice gradually decreasing during the melt season. Because of this heat flow superimposed ice forms at the level of impermeable ice, generally less than 0.1 m/year.~~The surface melt water does not percolate through the level of the winter cold wave. The heat flow into the ice is gradually decreasing during the melt season. Superimposed ice forms at the level of impermeable ice.~~

Formatted: Font: (Default) Times New Roman, 12 pt, Font color: Black, English (United Kingdom)

Formatted: Font: (Default) Times New Roman, 12 pt, Font color: Black, English (United Kingdom)

Formatted: Font: (Default) Times New Roman, 12 pt, Font color: Black, English (United Kingdom)

4.6 Radiocarbon dating

The AMS radiocarbon dating obtained from organic-rich layers and from carbonaceous aerosols embedded in clear ice in the Juvfonne ice patch shows ages spanning from modern at the surface to ca. ~~6200 BCE~~7600 cal. years BP at the bottom (clear ice below the basal organic-rich layer), thus showing that Juvfonne has existed continuously during the last ~7500 years~~yrs~~. So far, the basal ice in Juvfonne is the oldest dated ice in mainland Norway (Table 2)~~)~~.

In the tunnel opened in 2010 the AMS radiocarbon dating of organic matter embedded in the ice shows modern age in the top layer at the entrance, and ages ranging from ~~1218-1125~~3075-3168 cal. years BP~~ BCE~~ to ~~945-987 CE~~963-1005 cal. years BP inside the tunnel. These results were previously published in Nesje et al. (2012) and recalibrated for this study (~~Fig. 14~~Table 2 and Fig. 15).

In the tunnel opened in 2012 the AMS radiocarbon dating of five organic layers embedded in the ice about 70 m from the margin of the ice patch, yielded dates in chronological order from the base upwards, ranging from ~~4711-4606 BCE~~6556-6661 cal. years BP at the base to ~~53 BCE – 21 CE~~1971-2003 cal. years BP in the ceiling of the ice tunnel, approximately 2.8~~5~~ m above the tunnel floor. The organic debris that yielded the oldest age was collected from the innermost part of the ice tunnel, about 0.4~~3~~ m above the bed. The layer where the sample was retrieved could be followed close to the bed in the inner parts of the tunnel. The carbon dates on carbonaceous aerosols were sampled at the same location to the side and below the plant fragment layer~~ (Table 3).~~. The oldest dating is 7519-7670~~is 6418-5988 BCE~~ cal. years BP. The position of the sample site in the 2012 tunnel is marked on Fig. 3a.

In the autumn 2014, two *in-situ Polytrichum* moss mats melted out along the margin of Juvfonne south of the ice tunnel excavated in 2010. AMS radiocarbon dates of the two moss mats indicate that the moss was killed by the expanding margin of the ice patch about 2000 years ago (1951-1896 cal. years BP - Poz-66166 and 1945-1882 cal. years BP - Poz-66167)~~1 BCE -54 CE – Poz-66166 and 5-68 CE – Poz-66167)~~. ~~Thus~~Thus, the minimum extent of the south-eastern part of the ice patch observed in September 2014 is most likely the smallest in 2000 years.

With the exception of one identified outlier, the results obtained ~~results~~ from dating of carbonaceous aerosol particles in the ice could reproduce the expected ages very well (Zapf et al., 2013). This gives confidence that the age of organic debris in the ice is similar to the surrounding ice. In Fig.16 radiocarbon datings from both ice tunnels are plotted according to vertical distance from bed.

5 Discussion

The discussion focuses on the value of this research in the context of the long-term objective to develop models of mass balance and thermal regime on Holocene time scale at ice patches and surrounding terrain.

The discussion is organised in four sections: (1) the mass balance, (2) thermal regime, (3) ice layering and deformation on Holocene time scale and (4) the environmental processes relevant to artefact displacement and preservation.

5.1 The mass balance

Perennial ice patches are, due to their existence, located at sites with close to long-term zero mass balance. The inter-annual variability in summer and winter balance could be considerable, but the long-term changes in mass must be close to zero as long as they do not disappear or develop into a glacier. The 6-year record of mass balance gives some insight into the spatial and temporal variability of the mass balance.

The snow accumulation during the 6-year period (2010-2015) shows increased accumulation towards the front of the ice patch. This is probably a response to increased melt, which will increase the snow accumulation at the leeward side of prevailing westerly winds.

Along the outer rim of JuvfonneJuvfonne, the surface altitude changes (negative net balance) vary between less than 1m to nearly 5m within a 200 m distance at same altitude over a period of 3 years (Fig. 3d). Field data is consistent with the interpretation of increased melting due to sensible and latent heat fluxes. Micro-meteorological investigations by Mott et al. (2011) of processes driving snow ablation in an alpine catchment show that advection of sensible heat cause locally increased ablation rates at the upwind edges of the snow patches.

The 2010 anomaly in the summer balance (Fig. 7a) is most likely related to increased melt during periods with strong south and south-easterlysoutheasterly winds (unsheltered direction for Juvfonne) combined with relatively high air temperatures and high relative humidity causing enhanced turbulent fluxes. Extreme melt was observed in early-mid August. The warmest 10-day period in 2010 was 8-18 August. Median wind speed was 3.4 m/s from SE and humidity 79.5% at the meteorological station 750 m from the ice patch. This 2010 anomaly is probably the reason for the asymmetric net balance of Juvfonne (Fig. 6). Exceptionally large melt episodes have been reported from the Central Cascade Mountains of Oregon where snow melt were enhanced by strong wind, high air temperature and high humidity (Marks et al., 1998). At higher unsheltered sites 60-90% of the energy for snowmelt came from sensible and latent heat exchanges, while it was only about 35% at more sheltered sites. Recently similar extreme melt events have been reported from the southern and western part of Greenland ice sheet in July 2012, where nonradiative energy fluxes (sensible, latent, rain, and subsurface collectively) dominated the ablation area surface energy budget during multiday episodes (Fausto et al., 2016). Exceptionally large melt episodes have recently been reported from the southern and western part of Greenland ice sheet in July 2012, where

Formatted: Font: (Default) Times New Roman, 12 pt, Font color: Black, English (United Kingdom)

Formatted: English (United Kingdom)

Formatted: English (United States)

Formatted: Font color: Black, English (United States)

Formatted: Font: Not Italic, Font color: Black, English (United States)

Formatted: Font: Not Italic, Font color: Black, English (United States)

Formatted: Font: Not Italic, Font color: Black, English (United States)

Formatted: Font: Not Italic, Font color: Black, English (United States)

Formatted: Font color: Black, English (United States)

~~nonradiative energy fluxes (sensible, latent, rain, and subsurface collectively) dominated the ablation area surface energy budget during multiday episodes (Fausto et al., 2016).~~

The snow recording from the station in front of Juvfonne (95 m from the front) clearly illustrates the complexity of snow accumulation in this environment. In front of Juvfonne abrupt changes in snow depth within hours dominate the series, causing great day-to-day variability. These changes seem to be mainly driven by the rate of wind speed and wind direction. S~~One s~~ingle storm events with westerly winds could account for almost 50% of the winter accumulation in less than 24 hours, like the storm February 7-8 in 2015 ~~-~~(Fig.~~ure~~ 12~~1~~, 2014-15). Spring snow accumulation with insignificant wind drift could also influence mass balance, like the period from early April to mid May 2012 where more than 40 cm of snow accumulated (Fig. 12, 2011-2012).~~Spring snow accumulation with insignificant wind drift could also influence mass balance, like the 2012 season.~~

5.2 Ground and ice thermal regime

Formatted: Font color: Black, English (United States)

Formatted: Font color: Black, English (United States)

Formatted: Font: Not Italic, Font color: Black, English (United States)

Formatted: Font: Not Italic, Font color: Black, English (United States)

Formatted: Font: Not Italic, Font color: Black, English (United States)

Formatted: Font: Not Italic, Font color: Black, English (United States)

The temperature measurements at Juvfonne show that there is sufficient melt water to bring the permeable snowpack to an isothermal condition within a few weeks in early summer (Fig. 13). Below the seasonal snowpack, the ice remains cold during the summer with temperatures on the range -2 - -4°C at 5-10 m depth (Fig. 13). In Norway most glaciers are considered to be temperate, although measurements are available for only a few glaciers (Andreassen and Winswold, 2012). Recent observations from nearby glaciers in Jotunheimen, reveal that at the lower parts of Storbreen the winter cold wave is removed during summer, but remained at Hellstugubreen and Gråsubreen (Sørdal, 2013; Tachon, 2015). The temperature measured close to the equilibrium line at Hellstugubreen (-1°C) and Gråsubreen (-2°C) were warmer than the temperature measured at similar depths at Juvfonne (-3°C).

Juvfonne consists of cold ice surrounded by permafrost terrain (Fig. 13~~2~~). Perennial ice patches can be used as indicators of local (mountain) permafrost conditions (Imhof, 1996; Kneisel, 1998). The physical background is that their ice cannot warm above 0°C in summer, but cool down far below 0°C during the cold season. Holocene permafrost modelling (Lilleøren et al., 2012) suggest that permafrost survived the highest areas of the Scandinavian mountains during the Holocene thermal maximum (HTM), and thus permafrost ice could be of Pleistocene age. Radiocarbon dates from Juvfonne show that the deepest central part of the ice patch contains carbonaceous particles embedded in the ice 7519-7670 cal. years BP ~~6418-~~

~~5988 BCE~~ (JUV0_B~~5~~ - Table 2). This is a strong indication that Juvfonne has existed continuously since mid-Holocene, and the dating of the ice could offer strongly needed validation of Holocene permafrost models. Juvfonne could contain older ice, and it is most likely that ice patches at higher altitude contains older ice.

~~The thermal regime of the ice in Juvfonne is similar to what is found close to the equilibrium line of nearby glaciers~~ (Sørdal, 2013; Tachon, 2015)~~. The temperature measurements show that there is sufficient melt water to bring the permeable snowpack to an isothermal condition within a few weeks in early summer (Fig. 13). Below the seasonal snowpack, the ice remains cold during the summer with temperatures on the range -2 – -4°C at 5-10 m depth (Fig. 12).~~

5.3 Ice layering and deformation on Holocene time scale

The observed ice layers almost certainly represent surface of isochronic deposition. Within both ice tunnels in Juvfonne there are several organic/debris layers of uncertain origin. From the appearance of these layers, it is probably wind or water transported material or reindeer droppings. The organic layers are horizontally continuous over a few meters. There is reasonable correlation between the age of the clear ice and the age of the organic layers (Zapf et al., 2013). Contamination is not likely in the clear ice samples, which gives confidence in the dating of the ice stratigraphy. This is necessarily not the case at other ice patches, where surface processes or microbial activity may contaminate organic material exposed at the surface.

The ice deformation on Holocene time scale is difficult to calculate based on the available data. In the central parts of the ice patch, ~~a first order~~an estimate of maximum basal shear stress is on the range of 30-40~~5~~ kPa (~~no averaging of~~ surface slope 17º, depth 12-16 m, laminar flow). Adding 5 m to the depth will increase the basal shear stress to 45~~0-60~~ 55 kPa for the central part. The latter is probably close to the range for the last decades. Calculation of deformation based on a Glen type flow law will be highly sensitive to the chosen stress exponent (Glen, 1955). Using a softness parameter A=2.4*10^{-15} s^{-1} kPa^{-3} based on an ice temperature of -2 ºC from Table 5.2 in Paterson (1994) and a stress exponent of n=2 (Duval et al., 2000) gives a surface velocity of 2.3 m/1000*years (surface slope 17º, depth 19 m, laminar flow). A likely situation for the LIA (surface slope 15º, depth 45-60 m) gives an estimate of 25-60 m/1000*years assuming a cold based glacier (Fig. 16). These calculations are uncertain, but suggest that ~~The~~ a cumulative deformation of ice ~~(maximum ~30-60 kPa~~

Formatted: Font color: Black

basal shear stresses) over millennia could explains the observed curved layering in the basal layer of the ice patch (Fig. 4). The possibility of cCumulative ice deformation on a time scale of several millennia makes it difficult to relate the present thickness and slope of theses layers to previous thickness of the ice patch.

The observed ice layers almost certainly represent surface of isochronic deposition. Within both ice tunnels in Juvfonne there are several organic/debris layers of uncertain origin. From the appearance of these layers, it is probably wind or water transported material or reindeer droppings. In the case of Juvfonne, there is a reasonable correlation between the age of the ice and the age of the organic layers (Zapf et al., 2013). This is necessarily not the case at other ice patches.

The empirical relation between basal shear stress and altitude range of glaciers was investigated by Haeberli and Hoelzle (1995) based on data from the European Alps. A basal shear stress of 15-20 kPa is in good agreement with the values for ice bodies with elevation ranges of 150m as at Juvfonne.

5.4 Artefact displacement and preservation

From a cultural management perspective, there is particular interest in developing methods to identify sites of interest (Rogers et al., 2014) and a better understanding of the environmental threats (Callanan, 2015). The environmental threats are mainly related to sub-aerial exposure of artefacts. Especially leather artefacts, textiles and steering feathers of arrows are exposed to movement and decomposition short time after melt out. Wooden objects are more resistant.

The artefacts found at Juvfonne have been foundare in permafrost terrain surrounding the ice patch, most of them are found in the front of the ice patch within a few tens of meters of the ice patchmeters. The wooden artefacts range from 250-900 CE. Even during the extreme minimum in September 2014 (Fig. –6) there are no observations of artefacts melting out within the ice.

The exposure time to physical processes and microbial activity is critical to artefact decomposition. At JuvfonneJuvfonne, there is a gradual increase in the ground exposure time depending on snow accumulation and melt over millennia. The oldest ice found so far is 7519-7670 cal. years BP 6418-5988 BCE (JUV0_5 B - Table 2). At the eastern edge AMS radiocarbon dates show that the moss mats were covered (killed) by the expanding snowfield about 2000 years ago (Table 2, Poz-56952). Lichenometry indicates that the front of Juvfonne extended ~250 m from its present position during the LIA maximum in the mid-18th century (Nesje et al., 2012). A photo of Juvfonne from around 1900 shows the front close to the expected LIA extent (Fig. 16). These results constrain the extent of the ice patch since the mid-Holocene, but temporal and spatial variability need to be considered to assess the actual exposure time of artefacts.

Several radiocarbon dates of the top layer in 2010 (Fig. 4) show modern age. This means that artefacts found at Juvfonne have been sub-aerially exposed after the LIA but prior to 2009. ThusThus, the dating and position of artefacts cannot be used directly to reconstruct previous ice patch extent.

Juvfonne and surrounding terrain is an active environment in terms of geomorphological processes. In particular, during the extreme melting in autumn 2014 several small accumulations of organic material/debris occurred at the upper margin of the ice patch. Within a few days, melt water moved this material to the front of the ice patch. Downslope movement of artefacts by melt water is certainly possible at Juvfonne. Finds at other ice patches in Jotunheimen supports this interpretation, where different pieces of the same artefact have beenwas found along the direction of steepest slope. Textiles and leather objects are more likely transported by wind, and preservation at its original position is less likely. There are no finds of textiles or leather objects at Juvfonne.

6 Conclusions and future perspectives

The exploratory analyses of field data from Juvfonne show for the first time the geoscience research potential of ice patches in Scandinavia. The results give new insights into their age, internal structure, mass balance and climate sensitivity, and have taken the state of knowledge to level where models can be designed.

These are the main conclusions from the analysis of field data:

- Ice stratigraphic characteristics and radiocarbon dating strongly suggest that the Juvfonne ice patch was small or absent during Holocene thermal maximum, but existed continuously since ca. 7600 cal. years BP (the late Mesolithic period) without disappearing. This is the oldest dating of ice in mainland Norway.

- A 6-year record of mass balance measurements shows a strong negative balance. The total mass loss at one site was 10.5 m w.e. Elevation changes are highly asymmetric over short distances, from close to zero to surface lowering of several meters. There is a significant increase in snow accumulation towards the front of approx. 20% compared to the upper central area. The winter balance is poorly correlated with winter precipitation. One single storm event may contribute significantly to the winter balance.
- Temperature measurements of the ice in Juvfonne reveal colder ice than what is found at similar depths close to the equilibrium line of nearby polythermal glaciers. There is sufficient melt water to bring the permeable snowpack to an isothermal state within a few weeks in early summer. Below the seasonal snowpack, at 5-10 m depth, the ice remains cold with temperatures between -2 and -4°C. The cold ice is surrounded by permafrost terrain having similar ground temperatures.
- Geophysical investigations show a clear stratification. The observed ice layers almost certainly represent surface of isochronic deposition. At depth, curved reflection horizons are observed consistent with cumulative ice deformation over millennia.
- Ice deformation and surface processes (i.e. wind and melt water) may have caused significant displacement of artefacts from their original position.
- Since the surface ice shows modern age artefacts melted out in front of Juvfonne since 2009 have been sub-aerially exposed after the LIA but prior to 2009. Thus, the dating and position of artefacts cannot be used directly to reconstruct previous ice patch extent.

The radiocarbon datings show that Juvfonne is robust to climate change, even on a Holocene timescale. The datings indicate a slow build-up over a period of 8000 years. The survival of relatively thin ice over a long period is a good documentation of the well-known mass balance feedback mechanisms of ice patches. The datings of mass mats appearing at the southeastern edge of Juvfonne in September 2014 suggest the smallest ice patch in ~2000

Formatted: No bullets or numbering

years. These field data constrain the Holocene development of Juvfonne, but care should be taken in the interpretation. Radiocarbon datings only show the timing of minima in volume.

Perennial ice patches are, due to their existence, areas with close to long-term zero mass balance similar to the zone close to the ELA of glaciers. However, there are obvious differences between ice patches and glaciers. The accumulation processes are to a variable degree dependent on surrounding topography and the topography of the ice patch itself. One possible future approach is field observations in combination with numerical simulation of the wind field to obtain the necessary spatial and temporal resolution to model the snow accumulation during storm events. The wind field with high spatial and temporal resolution is also needed to calculate the turbulent fluxes.

Ice patches are in the transition zone between seasonal snow cover and perennial snow/ice. This interaction needs to be addressed since ice patches could be influenced by advective heat transfer in summer. The melt anomaly in 2010 is probably related to periods of strong southeasterly winds, high air temperatures and high relative moisture boosting the turbulent fluxes at the upwind edge. The time series of mass balance at Juvfonne is too short to study the long-term effect of melt anomalies.

Cumulative deformation of ice on a Holocene time scale m in the interpretation of the ice layering and makes it difficult to relate the present thickness and slope of theses layer to previous thickness of the ice patch. Maximum ice volume was reached during LIA, when Juvfonne probably developed into a cold based glacier with significant internal deformation.

~~Based on a 6-year field experiment on Juvfonne ice patch in central southern Norway, the following main conclusion could be drawn:~~

- ~~Ice stratigraphic characteristics and radiocarbon dating strongly suggest that the Juvfonne ice patch was small or absent during Holocene thermal maximum, but existed continuously since ca. 6200 BCE (the late Mesolithic period) without disappearing or developing into a glacier with basal sliding. The oldest radiocarbon dates show that the deepest central part of the ice patch contains carbonaceous particles embedded in the ice 6418-5988 BCE, which is the oldest dating of ice in mainland Norway.~~
- ~~Radiocarbon dates show that the moss mats appearing in 2014 were covered (killed) by the expanding snowfield about 2000 years ago. The minimum extent observed in~~

Formatted: Bulleted + Level: 1 + Aligned at: 0,63 cm + Indent at: 1,27 cm

September 2014 at the south-eastern part is most likely the smallest ice patch in ~2000 years.

- A 6-year record of mass balance measurements shows a strong negative balance. The total mass loss at one site was 10.5 m w.e. Elevation changes are highly asymmetric over short distances, from close to zero to surface lowering of several meters. There is a significant increase in snow accumulation towards the front of approx. 20% compared to the upper central area. Assuming that this is a close to equilibrium situation, increased accumulation reflects increased melt. Locally increased ablation rates are probably caused by significant spatial variability of the sensible and latent heat fluxes. The melt anomaly in 2010 is most likely related to periods of strong south-easterly winds and high relative moisture boosting the turbulent fluxes.
- The winter balance is poorly correlated with winter precipitation. One single storm events may contribute significantly to the winter balance.
- The thermal regime of the ice in Juvfonne is similar to what is found close to the equilibrium line of nearby glaciers. Temperature measurements show that there is sufficient melt water to bring the permeable snowpack to an isothermal state within a few weeks in early summer. Below the seasonal snowpack, at 5-10 m depth, the ice remains cold with temperatures between -2 and -4°C. The cold ice is surrounded by permafrost terrain having similar ground temperatures.
- Geophysical investigations show a clear stratification. The observed ice layers almost certainly represent surface of isochronic deposition. At depth, curved reflection horizons are observed consistent with cumulative ice deformation over millennia. Even a thin ice patch like Juvfonne (<20 m thick) ice deformation is a critical factor in the interpretation of the ice layering and makes it difficult to relate the present thickness and slope of theses layer to previous thickness of the ice patch.
- Ice deformation and surface processes (i.e. wind and melt water) may have caused significant displacement of artefacts from their original position.
- Artefacts melted out in front of Juvfonne since 2009 have been sub-aerially exposed after the LIA but prior to 2009. Thus the dating and position of artefacts cannot be used directly to reconstruct previous ice patch extent.

~~The exploratory analyses of field data from Juvfonne show for the first time the geoscience research potential of ice patches in Scandinavia. The results give new insights into their age, internal structure, mass balance and climate sensitivity, and have taken the state of knowledge to level where models can be designed. The feedback mechanisms observed on Juvfonne suggest that ice patches are robust to climate change, at least on the time scale of decades. Perennial ice patches are, due to their existence, areas with close to long-term zero mass balance. However, they are probably more sensitive than glaciers to changes in the wind pattern. In the perspective of surface energy and mass balance; ice patches are in the transition zone between permafrost terrain and glaciers. Future research will need to carefully address this interaction to build reliable models of how ice patches have developed during the Holocene and their response to future climate change.~~

Acknowledgements

We thank the archaeologists Lars Pilø and Espen Finstad for valuable comments and discussions related to artefact displacements and Dag Inge Bakke at Mimisbrunnr Klimapark 2469 for support in the field. Professor Emeritus Wilfried Haeberli and Professor Bernd Etzelmüller gave useful comments to an earlier version of the manuscript and are gratefully acknowledged. We thank two anonymous reviewers for precise feedback, which greatly improved the manuscript.

References

Andreassen, L. M.: Glaciological investigations in Norway in 2010 - Juvfonne, NVE report 3, B. Kjølmoen (ed), 54-57 pp., 2011.

Andreassen, L. M., Elvehøy, H., Kjøllmoen, B., Engeset, R. V., and Haakensen, N.: Glacier mass-balance and length variations in Norway, Ann Glaciol, 42, 317-325, 2005.

Andreassen, L. M., Paul, F., Kääb, A., and Hausberg, J. E.: Landsatderived glacier inventory for Jotunheimen, Norway, and deduced glacier changes since the 1930s, The Cryosphere, 2, 131-145, 2008.

Andreassen, L. M. and Winswold, S. H.: Inventory of Norwegian Glaciers, 236 pp. pp., 2012.

Andrews, T. D. and Mackay, G.: The Archaeology and Paleoecology of Alpine Ice Patches: A Global Perspective, ARCTIC, 65, 4 pp., 2012.

Bakke, J., Dahl, S. O., Paasche, Ø., Riis Simonsen, J., Kvisvik, B., Bakke, K., and Nesje, A.: A complete record of Holocene glacier variability at Austre Okstindbreen, northern Norway: an integratd approach, Quarternary Science Reviews, 29, 1246-1262, 2010.

Bronk Ramsey, C. and Lee, S.: Recent and Planned Developments of the Program OxCal, Radiocarbon, 55, 2013.

Brunswig, R. H.: Risks and Benefits of Global Warming and the Loss of Mountain Glaciers and Ice Patches to Archeological, Paleoclimate, and Paleoecology Resources, Ecological Questions, 20, 99-108, 2014.

Callanan, M.: Managing the frozen heritage: Some challenges and responses, Quarternary International, in press, 8 pp., 2015.

Callanan, M.: Northern Snow Patch Archaeology, Oxford2010.

Ceruti, C.: Human bodies as objects of dedication at Inca mountain shrines, north-western Argentina, World Archaeology, 36, 103-122, 2004.

Curry, A.: Racing the thaw, Science, 346, 157-159, 2014.

Dadic, R., Mott, R., Lehning, M., and Burlando, P.: Wind influenceonsnow depth distribution and accumulation over glaciers, J Geophys Res, 115, 8 pp., 2010.

Dixon, E. J., Callanan, M., Hafner, A., and Hare, G. P.: The Emergence og Glacial Archaelogy, Journal of Glacial Archaeology, 1, 1-9, 2014.

Dixon, J., Manley, W. E., and Lee, C. M.: The emerging archaeology of glaciers and ice patches, American Antiquity, 70, 129-143, 2005.

Duval, P., Arnaud, L., Brissaud, M., Montagnat, M., and de la Chapelle, S.: Deformation and recrystallization processes of ice from polar ice sheets, Annals of Glaciology, 30, 83-87, 2000.

Engeset, R. V., Tveito, O. E., Alfnes, E., Mengistu, Z., Udnæs, H.-C., Isaksen, K., and Førland, E. J.: Snow Map System for Norway, Tallinn, Estonia2004.

Essery, E., Ganger, R., and Pomeroy, J.: Boundary-layer growth and advection of heat over snow and soil patches: modelling and parameterization, Hydrol. Processes, 20, 953-967, 2006.

Eveland, J. W., Gooseff, M. N., Lampkin, D. J., Barrett, J. E., and D., T.-V. C.: Seasonal controls on snow distribution and aerial ablation at the snow patch and landscape scales McMurdo Dry Valleys, Antarctica, The Cryosphere, 7, 917–913, 2013.

Farbrot, H., Hipp, T., Etzelmuller, B., Isaken, K., Ødegård, R. S., Schuler, T. V., and Humlum, O.: Air and Ground Temperatures Variations Observed along Elevation and Continentality Gradients in Southern Norway, Permafrost Periglacial Processes, doi: 10.1002/ppp.733, 2011. 2011.

Farnell, R., Hare, G. P., Blake, E., Bowyer, V., Schweger, C., Greer, S., and Gotthardt, R., 2004. . Arctic 57(3), 247–259.: Multidisciplinary investigations of alpine ice patches in Southwest Yukon, Canada: paleo-environmental and paleobiological investigations, ARCTIC, 57, 247-259, 2004.

Fausto, R. S., van As, D., Box, J. E., Colgan, W., Langen, P. L., and Mottram, R. H.: The implication of nonradiative energy fluxes dominating Greenland ice sheet exceptional ablation area surface melt in 2012, Geophys. Res. Lett., 43, 10 pp., 2016.

Finstad, E. and Vedeler, M.: En bronsealdersko fra Jotunheimen, Viking, 71, 61-70, 2008.

Fujita, K., Hiyama, K., Iida, H., and Ageta, Y.: Self-regulated fluctuations in the ablation of a snow patch over four decades, Water Resour. Res., 46, 9, 2010.

Fukui, K.: Permafrost and surface movement of an active protalus rampart in the Kuranosuke Cirque, the Northern Japanese Alps, Permafrost Conference, Zurich, 2003.

Fukui, K. and Iida, H.: Flow of the ice body in the Gozenzawa perennial snow patch, the Tateyama Mountains, central Japan, 2011.

Gisnås, K., Etzelmuller, B., Farbrot, H., Schuler, T. V., and Westermann, S.: CryoGRID 1.0: Permafrost Distribution in Norway estimated by a Spatial Numerical Model, Permafrost Periglacial Processes, 24, 2-19, 2013.

Gisnås, K., Westermann, S., Schuler, T. V., Melvold, K., and Etzelmuller, B.: Small-scale variation of snow in a regional permafrost model, The Cryosphere Discuss., 9, 6661-6696, 2015.

Glazirin, G. E., Kodama, Y., and Ohata, T.: Stability of drifting snow-type perennial snow patches, Bull. Glaciol. Res., 21, 1-8, 2004.

Glen, J. W.: The creep of polycrystalline ice, Proc. R. Soc. Ser. A, 228, 519-538, 1955.

Grosjean, M., Suter, P. J., Trachsel, M., and Wanner, H.: Ice-borne prehistoric finds in the Swiss Alps reflect Holocene glacier fluctuations, J. Quat. Sci., 22, 203-207, 2007.

Haeberli, W., Frauenfelder, R., Kääb, A., and Wagner, S.: Characteristics and potential climatic significance of ‘‘miniature ice caps’’ (crest- and cornice-type low-altitude ice archives), J GLACIOL, 50, 129-136, 2004.

Haeberli, W. and Hoelzle, M.: Application of inventory data for estimating characteristics of and regional clirn.ate-change effects on mountain glaciers: a pilot study with the European Alps, J GLACIOL, 21, 206-212, 1995.

Hamran, S.-E., Øyan, M. J., and Kohler, J.: UWB radar profiling reveals glacier facies, Granada, Spain2009.

Hansen, J. P. H., Meldgaard, J., and Nordquist, J.: Qilakitsoq. De Grønlandske mumier fra 1400-tallet, Nuuk and Copenhagen: Grønlands Landsmuseum/Christian Ejlers' forlag, 1985.

Hare, G. P., Thomas, C. D., Topper, T. N., and Gotthardt, R. M.: The archaeology of Yukon ice patches: New artifacts, observations, and insights, ARCTIC, 65, SUPPL. 1, 118-135, 2012.

Harris, C., Arenson, L. U., Christiansen, H. H., Etzelmuller, B., Frauenfelder, R., Gruber, S., Haeberli, W., Hauck, C., Holzle, M., Humlum, O., Isaksen, K., Kaab, A., Kern-Lutschg, M. A., Lehning, M., Matsuoka, N., Murton, J. B., Nozli, J., Phillips, M., Ross, N., Seppala, M., Springman, S. M., and Muhll, D. V.: Permafrost and climate in Europe: Monitoring and modelling thermal, geomorphological and geotechnical responses, Earth Sci. Rev., 92, 117-171, 2009.

Hauck, C., Isaksen, K., Vonder Mühll, D., and Sollid, J. L.: Geophysical surveys designed to delineate the altitudinal limit of mountain permafrost: an example from Jotunheimen, Norway, Permafrost Periglac, 15, 191-205, 2004.

Hipp, T., Etzelmuller, B., Farbrot, H., Schuler, D. V., and Westermann, S.: Modelling borehole temperatures in Southern Norway – insights into permafrost dynamics during the 20th and 21st century, Cryosphere, 6, 553-571, 2012.

Huss, M. and Fischer, M.: Sensitivity of Very Small Glaciers in the Swiss Alps to Future Climate Change, Front. Earth Sci., 4, 17 pp., 2016.

Imhof, M.: Modelling and Verification of the Permafrost Distribution in the Bernese Alps (Western Switzerland) Permafrost Periglac, 7, 267-280, 1996.

Isaksen, K., Hauck, C., Gudevang, E., Ødegård, R. S., and Sollid, J. L.: Mountain permafrost distribution on Dovrefjell and Jotunheimen, southern Norway, based on BTS and DC resistivity tomography data, Norsk Geografisk Tidsskrift, 56, 122-136, 2002.

Isaksen, K., Heggem, E. S. F., Bakkehøi, S., Ødegård, R. S., Eiken, T., Etzelmüller, B., and Sollid, J. L.: Mountain permafrost and energy balance on Juvvasshøe, southern Norway, In Proceedings Volume 1, Eight International Conference on Permafrost, Zurich, Switzerland, 21–25 July, 2003. 467-472, 2003.

Isaksen, K., Ødegård, R. S., Etzelmuller, B., Hilbich, C., Hauck, C., Farbrot, H., Eiken, T., Hygen, H. O., and Hipp, T.: Degrading mountain permafrost in southern Norway - spatial and temporal variability of mean ground temperatures 1999-2009, Permafrost Periglacial Processes, 22, 361-377, 2011.

Jenk, T. M., Szidat, S., Bolius, D., Sigl, M., Gäggeler, H. W., Wacker, L., Ruff, M., Barbante, C., Boutron, C. F., and Schwikowski, M.: A novel radiocarbon dating technique applied to an ice core from the Alps indicating late Pleistocene ages, J. Geophys. Res., 114, 2009.

Jenk, T. M., Szidat, S., Schwikowski, M., Gaggeler, H. W., Wacher, L., Synal, H.-A., and Sauer, M.: Microgram level radiocarbon (14C) determination on carbonaceous particles in ice, Nuclear Instruments and Methods in Physics Research B 259, 518-525, 2007.

Kawasaki, K., Yamada, T., and Wakahama, G.: Investigation of internal structure and transformational processes from firn and ice in a perennial snow patch, Ann Glaciol, 18, 117-122, 1993.

Kjøllmoen, B., Andreasse, L. M., Elvehøy, H., Jackson, M., and Giesen, R. H.: Glaciological investigations in Norway 2010, 106 pp. pp., 2011.

Kneisel, C.: Occurrence of surface ice and ground ice/permafrost in recently deglaciated glacier forefields, St. Moritz area, Eastern Swiss Alps, Yellowknife, Canada1998, 575-581.

Laumann, T. and Reeh, N.: Sensitivity to climate change of the mass balance of glaciers in southern Norway, J GLACIOL, 39, 656-665, 1993.

Lee, C. M.: Withering snow and ice in the mid-latitudes: A new archaeological and paleobiological record for the Rocky Mountain region, ARCTIC, 2012. 165-177, 2012.

Lehning, M., Löwe, H., Ryser, M., and Raderschall, N.: Inhomogeneous precipitation distribution and snow transport in steep terrain, Water Resour. Res., 44, 19 pp., 2008.

Lilleøren, K., Etzelmuller, B., Schuler, D. V., Gisnås, K., and Humlum, O.: The relative age of mountain permafrost - estimation of Holocene permafrost limits in Norway Global Planet. Change, 92-93, 209-223, 2012.

Marks, D., Kimball, J., Tingey, D., and Link, T.: The sensitivity of snowmelt processes to climate conditions and forest cover during rain-on-snow: a case study of the 1996 Pacific Northwest flood, Hydrol. Processes, 12, 1569-1587, 1998.

Matthews, J. A. and Dresser, P. Q.: Holocene glacier variation chronology of the Smørstabbtinden massif, Jotunheimen, southern Norway, and the recognition of century- to millennial-scale European Neoglacial events, The Holocene, 18, 181-201, 2008.

Meulendyk, T., Moorman, B. J., Andrews, T. A., and Mackay, G.: Morphology and Development of Ice Patches in Northwest Territories, Canada, ARCTIC, 65, SUPPL. 1, 43-58, 2012.

Morris, E. M.: Turbulent Transfer over Snow and Ice, Journal of Hydrology, 105, 205-223, 1989.

Mott, R., Daniels, M., and Lehning, M.: Atmospheric Flow Development and Associated Changes in Turbulent Sensible Heat Flux over Patchy Mountain Snow Cover, J Hydrometeorol, 16, 1315-1340, 2015.

Mott, R., Egli, L., Grunewald, T., Dawes, N., Manes, C., Bavay, M., and Lehning, M.: Micrometeorological processes driving snow ablation in an Alpine catchment, The Cryosphere, 5, 1083-1098, 2011.

Nesje, A.: Latest Pleistocene and Holocene alpine glacier fluctuations in Scandinavia. , Quarternary Science Reviews, 28, 2119-2136, 2009.

Nesje, A., Pilø, L. H., Finstand, E., Solli, B., Wangen, V., Ødegård, R. S., Isaken, K., Støren, E., Bakke, D. I., and Andreasse, L. M.: The climatic significance of artefacts related to prehistoric reindeer hunting exposed at melting ice patches in southern Norway, The Holocene, 22, 485-496, 2012.

Paterson, W. S. B.: The Physics of Glaciers, Pergamon, 1994.

Pohl, S., Marsh, P., and Liston, G. E.: Spatial-Temporal Variability in Turbulent Fluxes during Spring Snowmelt, ARCT ANTARCT ALP RES, 38, 136-146, 2006.

Reckin, R.: Ice Patch Archaeology in Global Perspective: Archaeological Discoveries from Alpine Ice Patches Worldwide and Their Relationship with Paleoclimates, Journal of World Prehistory, 26, 63 pp., 2013.

Reimer, P. J., Barad, E., Baykuss, A., Beck, J. W., Blackwell, P. G., Bronk Ramsey, C., Buck, C. E., Cheng, H., Edwards, R. L., Friedrich, M., Grootes, P. M., Guilderson, T. P., Haflidason, H., Hajdas, I., Hatte, C., Heaton, T. J., Hoffmann, D. L., Hogg, A. G., Hughen, K. A., Kaiser, K. F., Kromer, B., Manning, S. W., Niu, M., Reimer, R. W., Richards, D. A., Scott, E. M., Southhon, J. R., Staff, R. A., Turney, C. S. M., and van der Plicht, J.: IntCal13 and Marine13 radiocarbon age calibration curves 0-50,000 years cal BP, Radiocarbon, 55, 1869-1887, 2013.

Rogers, S. R., Fischer, M., and Huss, M.: Combining glaciological and archaeological methods for gauging glacial archaeological potential, Journal of Archaeological Science, 52, 410-420, 2014.

Ruff, M., Fahrni, S., Gäggeler, H. W., Hajdas, I., Suter, M., Synal, H.-A., Szidat, S., and Wacker, L.: On-line radiocarbon measurements of small samples using elemental analyzer and MICADAS gas ion source, Radiocarbon, 52, 1645-1656, 2010.

Saloranto, T. M.: Simulating snow maps for Norway: description and statistical evaluation of the seNorge snow model, The Cryosphere, 6, 1323-1337, 2012.

Sato, A., Takahashi, S., Naruse, R., and Wakahama, G.: Ablation and Heat Balance of the Yukikabe Snow Patch in the Daisetsu Mountains, Hokkaido, Japan, Annals of Glaciology, 5, 122-126, 1984.

Sigl, M., Jenk, T. M., Kellerhals, T., Szidat, S., Gaggeler, H. W., Wacher, L., Synal, H.-A., Boutron, C., Barbante, C., Gabrieli, J., and Schwikowski, M.: Towards radiocarbon dating og ice cores, Journal of Glaciology, 55, 985-996, 2009.

Sollid, J. L., Holmlund, P., Isaksen, K., and Harris, C.: Deep permafrost boreholes in western Svalbard, northern Sweden and southern Norway, Norwegian Journal of Geography 54, 186–191, 2000.

Spindler, K.: The Man in the Ice: The Preserved Body of a Neolithic Man Reveals the Secrets of the Stone Age, Sutton, Stroud, 1994.

Suter, P. J., Hafner, A., and Glauser, K.: Lenk – Schnidejoch. Funde aus dem Eis – ein vor- und frühgeschichtliche Passübergang. , Archäologie im Kanton Bern, 6B, 499-516, 2005.

Sørdal, I.: Kartlegging av temperaturtilhøva i Gråsubreen og Juvfonne. , Master, Department of Geosciences, University of Oslo, Oslo, 81 pp.+ app. pp., 2013.

Tachon, M.: Thermal regimes and horizontal surface velocities on Hellstugubreen and Storbreen, Jotunheimen, Southern Norway, Master, Department of Geosciences, University of Oslo, Oslo, 99 pp. + app. pp., 2015.

UNESCO: Perennial ice and snow masses – a guide for compilation and assemblage of data for the World Glacier Inventory, Technical Papers in Hydrology, 1, 1970.

Vedeler, M. and Jørgensen, L. B.: Out of the Norwegian glaciers: Lendbreen—a tunic from the early first millennium AD, Antiquity, 87, 788-801, 2013.

Westermann, S., Schuler, T. V., Gisnås, K., and Etzelmuller, B.: Transient thermal modeling of permafrost conditons in Southern Norway, The Cryosphere, 7, 719-739, 2013.

Winsvold, S. H., Andreassen, L. M., and Kienholz, C.: Glacier area and length changes in Norway from repeat inventories, The Cryosphere, 8, 1885-1903, 2014.

Zapf, A., Nesje, A., Szidat, S., Wacker, L., and Schwikowski, M.: 14C measurements of ice samples from the Juvfonne ice tunnel, Jotunheimen, Southern Norway—validation of a 14C dating technique for glacier ice, Radiocarbon 55, 571-578, 2013.

Zhang, Y. L., Perron, N., Ciobanu, V. G., Zotter, P., Minguillón, M. C., Wacker, L., Prévôt, A. S. H., Baltensperger, U., and Szidat, S.: On the isolation of OC and EC and the optimal strategy of radiocarbon-based source apportionment of carbonaceous aerosols, Atmos. Chem. Phys., 12, 10841-10856, 2012.

Ødegård, R.: Ground and glacier thermal regimes related to periglacial and glacial processes: Case studies from Svalbard and southern Norway, 2 Dr.Scient., Dr. scient. thesis (in English), Department of Geography, Rapportserie i naturgeografi, University of Oslo, Norway., Oslo, 44 pp. pp., 1993.

Ødegård, R., Nesje, A., Isaken, K., and Eiken, T.: Perennial ice patch studies – preliminary results from a case study in Jotunheimen, southern Norway, Geophysical Research Abstracts Vol. 13, EGU2011-12027, Vienna2011, 1.

Table 1.

Areal extents of Juvfonne derived from topographic maps, Landsat imagery, GNSS measurements by foot and digitising from orthohotos. *Seasonal snow remaining along the extent.

Year	Date	Source	Area (km^2)
1981		map	0.171
1984	10.08.1984	Orthophoto	0.208
1997	15.08.1997	Landsat	0.208
2003	09.08.2013	Landsat	0.150
2004	12.08.2004	map	0.187
2010	25.08.2010	GNSS	0.149
2011	02.08.2011	GNSS	0.150
2011	17.09.2011	Orthophoto	0.127
2012	12.09.2012	GNSS	0.160
2013	12.08.2013	GNSS	0.151
2014	09.09.2014	GNSS	0.101
2015	11.09.2015	GNSS	0.186*

Table 2. R~~ AMS r~~adiocarbon dates from the ice tunnels and ice samples from ice patch surface. Ages obtained by radiocarbon dating of clear ice and organic remains collected in the ice tunnels and from the ice patch surface. Ice samples were collected as blocks and subdivided in several sub-samples. Therefore an average value is shown for every block (JUV1, JUV2 and JUV3) except for JUV0, because JUV0_1 and JUV0_2 were taken adjacent to the plant fragment layer, dated 6600 cal BP (Poz-56955), while samples from JUV0_3 to JUV0_8 were collected at the bottom of the wall, a few cm below the plant fragment layer. Thus JUV0_A is the average of JUV0_1 and JUV0_2, while the other six samples were averaged as JUV0_B. Individual calibrated ages for ice sub-samples are not shown because derived ages were combined using the function in OxCal v4.2.4. (^{14}C date combination). Calibrated ages are given in years before present (cal BP, with BP = 1950) as median probability and 1 σ uncertainty range.

Sample ID	**AMS Lab. No.**	**Type of material**	**^{14}C age (BP)**	**cal age (cal BP)**	**median probability (cal BP)**
JUV3_1 (tunnel 2010)	ETH 42845.1.1	Surface ice	-940 ± 91	-	-
JUV3_2 (tunnel 2010)	ETH 42847.1.1	Surface ice	-720 ± 110	-	-
JUV3_3 (tunnel 2010)	ETH 42849.1.1	Surface ice	-1160 ± 100	-	-
JUV3_4 (tunnel 2010)	ETH 43446.1.1	Surface ice	-1220 ± 120	-	-
JUV3 (tunnel 2010)		Surface ice	-996 ± 52	(-45 - -42)	-43
JUV2_1 (tunnel 2010)	ETH 43443.1.1	Ice	1020 ± 210	-	-
JUV2_2 (tunnel 2010)	ETH 43445.1.1	Ice	1870 ± 670	-	-
JUV2_3 (tunnel 2010)	ETH 43559.1.1	Ice	1120 ± 320	-	-
JUV2_4 (tunnel 2010)	ETH 45109.1.1	Ice	1130 ± 280	-	-
JUV2 (tunnel 2010)		Ice	1116 ± 146	(918–1237)	1044
Poz-37877 (tunnel 2010)	Poz-37877	Organic remains	1095 ± 30	(963 - 1005)	1001
Poz-37879 (tunnel 2010)	Poz-37879	Organic remains	1420 ± 30	(1299 - 1338)	1322
Poz-39788 (tunnel 2010)	Poz-39788	Reindeer dung	1480 ± 30	(1336 - 1393)	1363
Poz-37878 (tunnel 2010)	Poz-37878	Organic remains	1535 ± 30	(1381 - 1418)	1438
Poz-56952 (tunnel 2012)	Poz-56952	Organic remains	2025 ± 30	(1971 - 2003)	1974
JUV1_3 (tunnel 2010)	ETH 43555.1.1	Ice	2144 ± 300	-	-
JUV1_4 (tunnel 2010)	ETH 43557.1.1	Ice	2650 ± 710	-	-
JUV1 (tunnel 2010)		Ice	2227 ± 277	(1904–2697)	2255
Poz-36460(tunnel 2010)	Poz-36460	Organic remains	2960 ± 30	(3075 - 3168)	3121
Poz-56953 (tunnel 2012)	Poz-56953	Organic remains	3490 ± 35	(3717 - 3781)	3764
Poz-56954 (tunnel 2012)	Poz-56954	Organic remains	4595 ± 35	(5290 - 5326)	5316

Tra-4427 (tunnel 2012)	Tra-4427	Organic remains	5044 ± 100	(5711 - 5904)	5791
Poz-56955 (tunnel 2012)	Poz-56955	Organic remains	5800 ± 40	(6556 - 6661)	6600
JUV0_1 (tunnel 2010)	BE 4184.1.1	Ice	5905 ± 248	-	-
JUV0_2 (tunnel 2010)	BE 4380.1.1	Ice	6293 ± 137	-	-
JUV0_A (tunnel 2012)		Ice	6207 ± 120	(6969 - 7255)	7099
JUV0_3 (tunnel 2012)	BE 4185.1.1	Ice	6512 ± 216	-	-
JUV0_4 (tunnel 2012)	BE 4381.1.1	Ice	6555 ± 133	-	-
JUV0_5 (tunnel 2012)	BE 4186.1.1	Ice	7296 ± 231	-	-
JUV0_6 (tunnel 2012)	BE 4382.1.1	Ice	6626 ± 196	-	-
JUV0_7 (tunnel 2012)	BE 4187.1.1	Ice	7285 ± 218	-	-
JUV0_8 (tunnel 2012)	BE 4383.1.1	Ice	6396 ± 229	-	-
JUV0_B (tunnel 2012)		Ice	6741 ± 79	(7519 - 7670)	7602

Formatted: German (Germany)

Ice tunnel 1 (opened 2010)

				Calibrated ages	
Lab. no.	Dated material	Radiocarbon age BP	Median probability	1 sigma (68.3%)	2 sigma (95.4%)
Poz-37877	Organic remains	1095 ± 30	CE 949	CE 945-987	CE 890-1012
Poz-37879	Organic remains	1420 ± 30	CE 627	CE 612-651	CE 582-660
Poz-39788	Reindeer dung	1480 ± 30	CE 586	CE 557-614	CE 539-644
Poz-37878	Organic remains	1535 ± 30	CE 511	CE 532-569	CE 428-592
Poz-36460	Organic remains	2960 ± 30	BCE 1172	BCE 1218-1125	BCE 1262-1072

……………………………………………………………………………………………………

Radiocarbon dates on carbonaceous aerosols trapped in the 'clean' ice matrix (Paul Scherrer Institute, Villigen, Switzerland; Zapf et al., 2013: Radiocarbon 55 (2-3), 571-578)

Formatted: English (United States)

		Calibrated ages BP (=AD 1950)		
Lab. no.	Radiocarbon age	Median probability	1 sigma (68.3%)	Comments
JUV3_1 42845.1	-940 ± 95 BP	-42 BP (1950)	-42 - -47 BP	Sample from ice patch surface
JUV3_2 42845.2	-723 ± 113 BP	-48 BP	-46 - -53 BP	Sample from ice patch surface
JUV3_3 42845.3	-1157 ± 102 BP	-36 BP	-8 - -42 BP	Sample from ice patch surface
JUV3_4 42845.4	-1221 ± 116 BP	-34 BP	-8 - -41 BP	Sample from ice patch surface
JUV-3 2010 mean	-1010 ± 107 BP	-41 BP	-40 - -45 BP (Modern)	Samples from ice patch surface

			Calibrated ages	
Lab. no.	Radiocarbon age BP	Median probability	1 sigma (68.3%)	2 sigma (95.4%)
JUV2_1 43443.1	1021 ± 205	CE 995	CE 861-1211	CE 640-1312
JUV2_2 43443.2	1874 ± 665	CE 45	BCE 592-CE 724	BCE 1433-CE 1329
JUV2_3 43443.3	1121 ± 321	CE 891	CE 640-1221	CE 251-1432
JUV2_4 43443.4	1126 ± 284	CE 892	CE 652-1169	CE 381-1405
JUV2 2010 Mean	1286 ± 409	CE 720	CE 378-1165	BCE 169-1442
JUV1_1/2 43442.1	3875 ± 342	BCE 2353	BCE 2776-1924	BCE 3138-1501
JUV1_3 43442.2	2144 ± 303	BCE 200	BCE 541-CE 172	BCE 846-CE 475
JUV1_4 43442.3	2647 ± 711	BCE 834	BCE 1641-CE 69	BCE 2588-CE 775
JUV1 2010 Mean	2889 ± 488	BCE 1105	BCE 1643-471	BCE 2346-CE 85

Ice tunnel 2 (opened 2012)

				Calibrated ages	
Lab. no.	Dated material	Radiocarbon age BP	Median probability	1 sigma (68.3%)	2 sigma (95.4%)
Poz-56952	Organic remains	2025 ± 30	BCE 25	BCE 53-BCE 21	BCE 111-CE 55
Poz-56953	Organic remains	3490 ± 35	BCE 1816	BCE 1831-1767	BCE 1904-1737
Poz-56954	Organic remains	4595 ± 35	BCE 3367	BCE 3376-3340	BCE 3382-3326
Tra-4427	Organic remains	5044 ± 100	BCE 3841	BCE 3954-3761	BCE 4001-3645
Poz-56955	Organic remains	5800 ± 40	BCE 4651	BCE 4711-4606	BCE 4729-4544

……………………………………………………………………………………………………

Radiocarbon dates on carbonaceous aerosols trapped in the 'clean' ice matrix sampled and dated in 2015 (Paul Scherrer Institute, Villigen, Switzerland)

Formatted: English (United States)

			Calibrated ages	
Lab. no.	Radiocarbon age BP	Median probability	1 sigma (68.3%)	2 sigma (95.4%)
juv1-1 4184.1.1	5909 ± 248	BCE 4807	BCE 5061-4495	BCE 5373-4319
juv1-2 4380.1.1	6300 ± 138	BCE 5255	BCE 5384-5203	BCE 5525-4932
juv2-1 4185.1.1	6521 ± 217	BCE 5455	BCE 5664-5292	BCE 5877-4985
juv2-2 4381.1.1	6565 ± 135	BCE 5514	BCE 5628-5463	BCE 5730-5293

juv3-1 4186.1.1	7306 ± 232	BCE 6178	BCE 6418-5988	BCE 6602-5725
juv3-2 4382.1.1	6682 ± 227	BCE 5609	BCE 5812-5463	BCE 6049-5207
juv5-1 4187.1.1	7293 ± 219	BCE 6166	BCE 6397-5987	BCE 6532-5734
juv5-2 4383.1.1	6405 ± 230	BCE 5336	BCE 5564-5204	BCE 5735-4800
juv 0 (2015) Mean	6623 ± 210	BCE 5555	BCE 5733-5359	BCE 5983-5206

~~Table 3.~~

~~Sample blocks~~	~~Sample description~~
~~1~~	~~JUV 0_1 and JUV 0_2: the side of the ice step with plant fragment layer. Clear ice divided into two sub samples.~~
	~~Since there was no place to cut off further ice, the other samples were taken from the wall on the left side of the corner where the ice step is located.~~
~~2~~	~~JUV 0_3 and JUV 0_4: divided into two subsamples. This sample broke into pieces during cutting, but it is clear ice.~~
~~3~~	~~JUV 0_5 and JUV 0_6: nice and clear ice block cut at the right of sample 4. It was divided into two subsamples.~~
~~4~~	~~This ice block contains a lot of dark organic material. For the moment it is stored in the cold room and has not been processed. It could be measured with the conventional radiocarbon procedure and it is possible to separate some clear ice for the carbonaceous dating approach.~~
~~5~~	~~JUV 0_7 and JUV 0_8: clear ice cut inside the hole left after cutting sample 3. It was divided intp two subsamples.~~

Formatted: Justified, Space Before: 6 pt, Line spacing: 1,5 lines

Formatted: Justified, Space Before: 6 pt, Line spacing: 1,5 lines

Formatted: Justified, Space Before: 6 pt, Line spacing: 1,5 lines

Formatted: Justified, Space Before: 6 pt, Line spacing: 1,5 lines

Formatted: Justified, Space Before: 6 pt, Line spacing: 1,5 lines

Formatted: Justified, Space Before: 6 pt, Line spacing: 1,5 lines

Formatted: Justified, Space Before: 6 pt, Line spacing: 1,5 lines

Table 4

Key statistics for the first order polynomial fit of snow accumulation (deviation from mean each year) in the period 2010-2015.

Sources of variation	Sums of squares	Degrees of freedom	Mean Square	F-test
First order polynomial regression	0.656	2	0.328	6.339
Deviation	11.847	232-2-1 (229)	0.052	
Total variation	12.503	232-1 (231)	0.054	

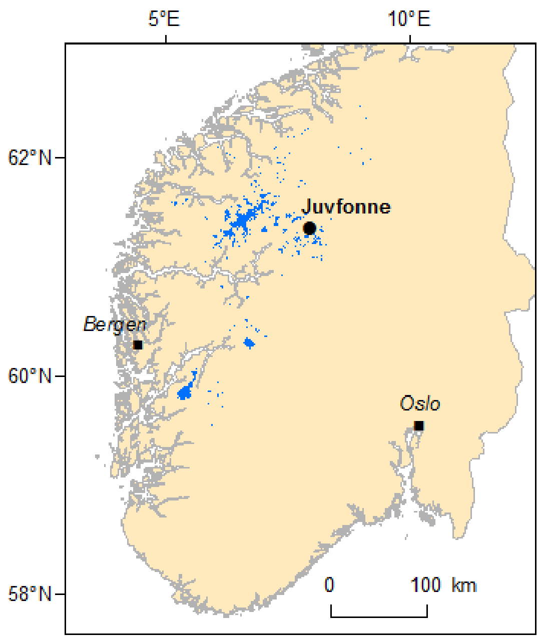

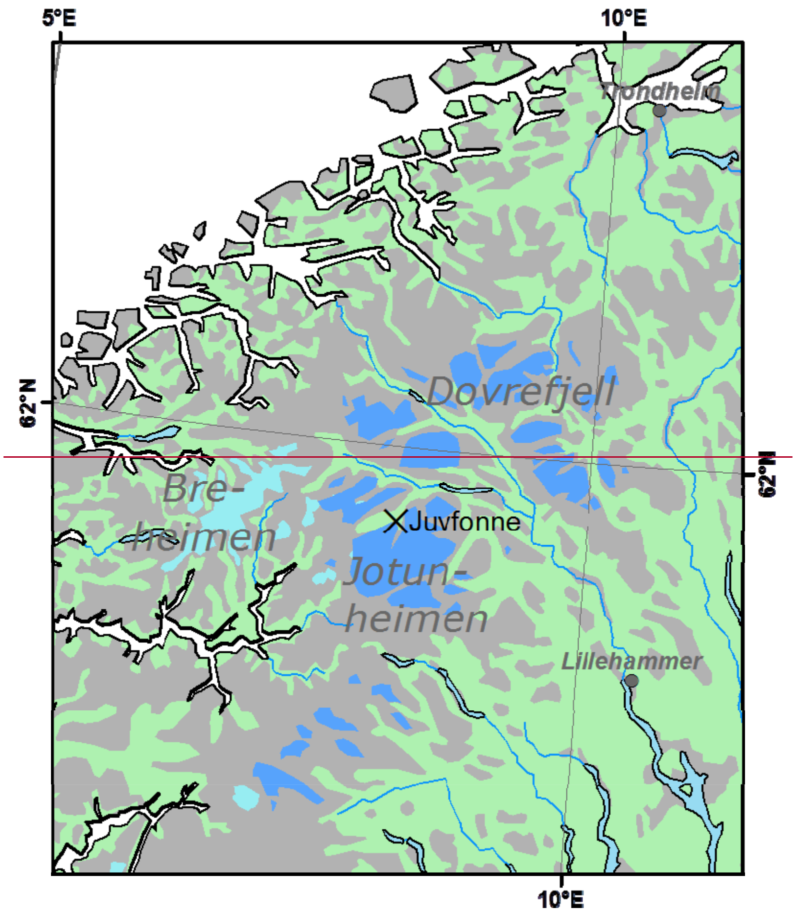

Figure 1. The field site Juvfonne ~~(marked with X)~~ in central southern Norway. Dark blue ~~is permafrost~~ areas~~, light blue is~~ are glaciers. ~~Permafrost extent generalized from Lilleøren et al. (2012).~~

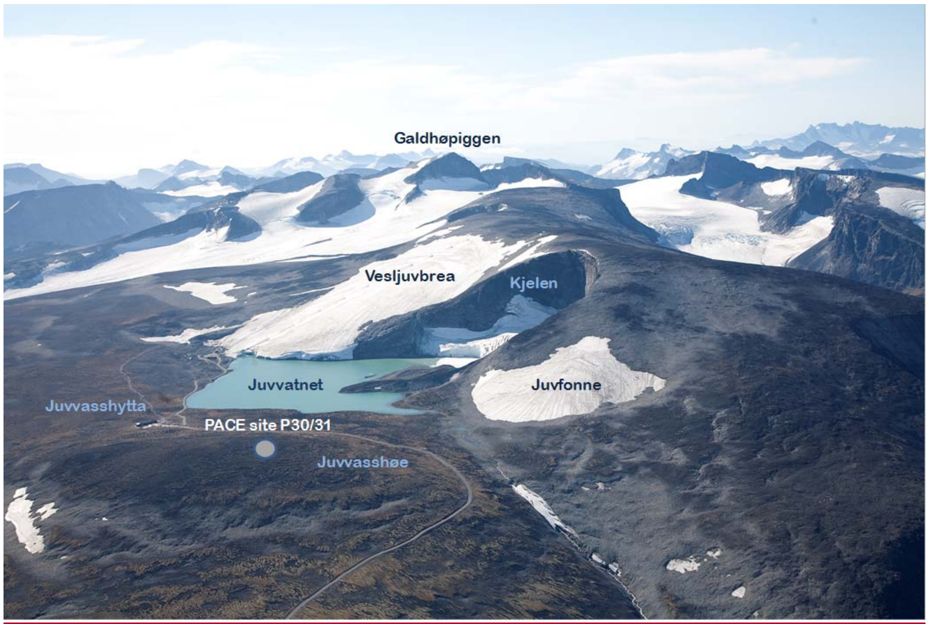
Galdhøpiggen
Vesljuvbrea
Kjelen
Juvvatnet
Juvfonne
Juvvasshytta
PACE site P30/31
Juvvasshøe


Galdhøpiggen
Vesljuvbrea
Kjelen
Juvvatnet
Juvfonne
Juvvasshytta
Juvvasshøe

Figure 2. Overview picture from September 2008 towards SSW showing~~of~~ Juvfonne and the Juvflye area including Kjelen, ~~-~~ Juvvatnet, Juvvasshytta, ~~Vesljuvbreen~~ Vesljuvbrea and the P30/ ~~and~~ 31 Permafrost and Climate in Europe (PACE) boreholes at Juvvasshøe. Also visible is the highest mountain of Norway, Galdhøpiggen (2469 m a.s.l.). Photo: Helge J. Standal.

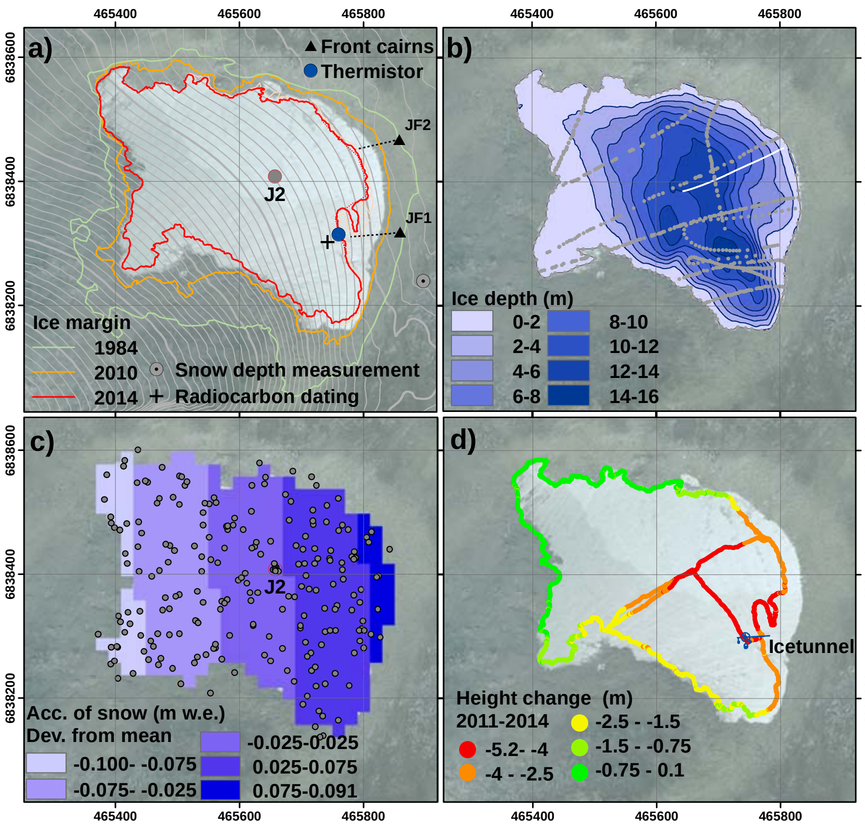

Figure 3. Maps of Juvfonne with ~~ortofoto~~orthophoto from September 2011 as background, a) ice margins, position of front measurements (JF1 and JF2- see ~~figure~~ Fig. 9~~14~~), position of mass balance stake J2, position of thermistor for ice temperature measurements (Fig. 1~~3~~2) and position of the oldest radiocarbon dating and position of snow depth measurement station, b) interpolated contours of bed topography relative to ice thickness in September 2011 (grey markers are ~~radarpoints~~radar points used in the interpolation) and position of the georadar track in Fig. 4 - white line, c) grey markers are snow depth measurements (2010-2015), the raster map shows a first order polynomial fit to the deviation from mean accumulation each year ~~(see table 3 for details)~~ d) height differences along GNSS tracks in 2014 relative to ice surface from laserdata in 2011 and positions of ice tunnel excavated in 2012.

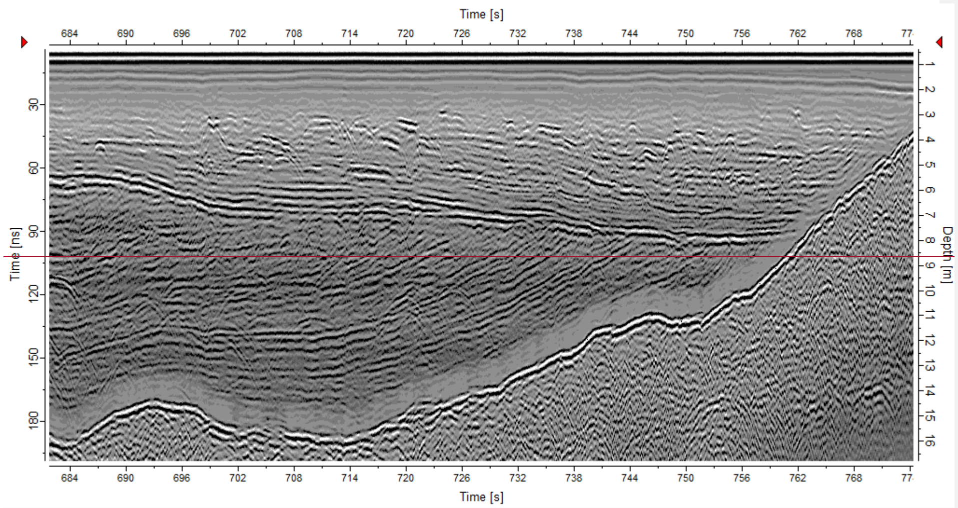

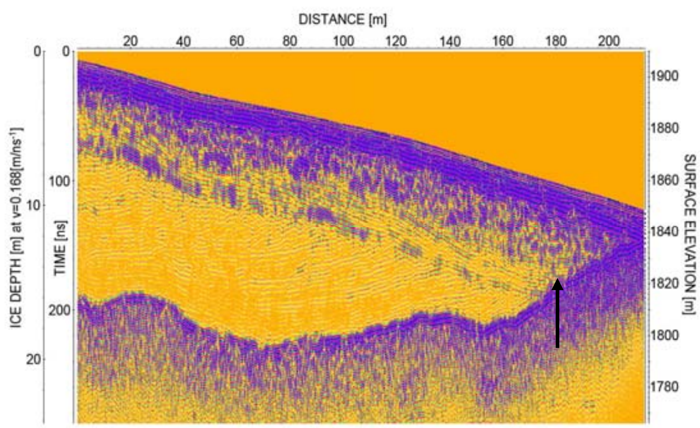

Figure 4. Example of ~~500~~ 250 MHz Georadar profile. The position of the track shown in ~~figure~~ Fig. 3b. The arrow shows the approximate minimum front position in September 2014

~~(Ice velocity: 168 m µs-1, adjustment velocity: 300 m µs-1, automatic gain control, scale factor 5000).~~.

Figure 5. Photo of angular discontinuity at the wall of the 2010 ice tunnel, as also observed on the georadar data (Fig. 4). The upper layering is parallel to the surface of Juvfonne. Radiocarbon dating of the upper part showed modern age. Width of picture is approximately 0.4 m.

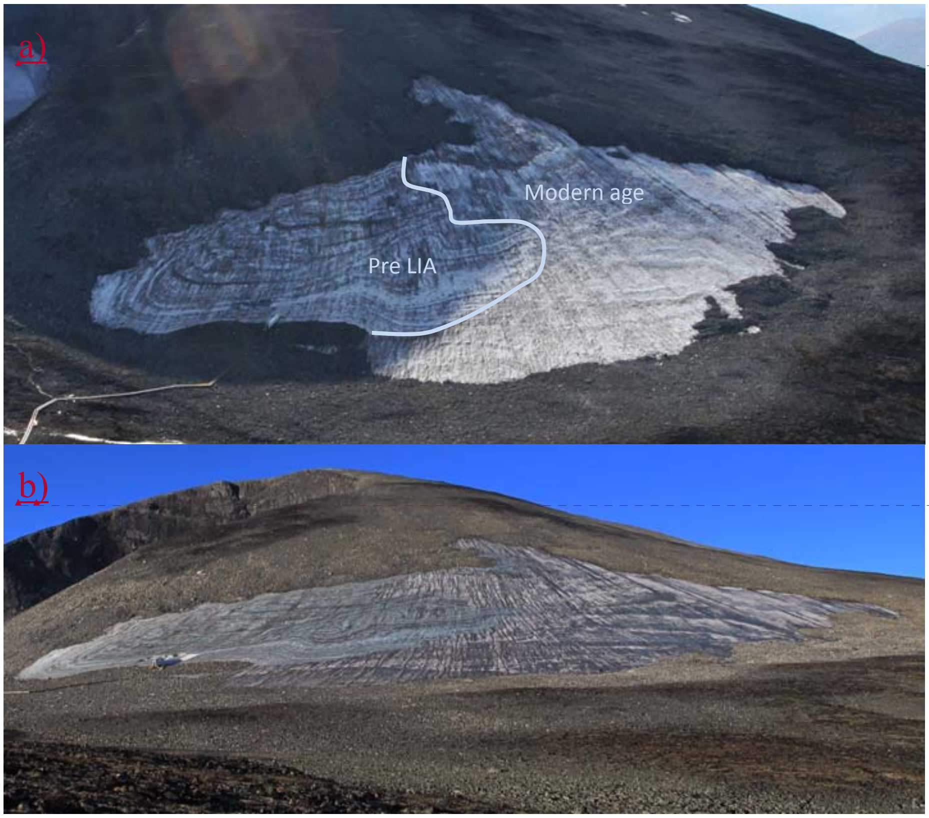

Formatted: Font: 18 pt, Font color: White

Formatted: Font: 18 pt

Formatted: Font: 18 pt, Font color: White

Figure 6. Photos of Juvfonne 17 September 2014 (a~~upper~~) and 10 September 2014 (b~~lower~~) showing the pre ~~'Little Ace Age'~~LIA surface exposed in central and southern parts of the ice patch (left side). The area on Juvfonne in the north-west (right side) is interpreted to be ice of modern age. The entrance of the ice tunnel is sitting on a small ridge that might be ice cored (left side lower image). The collapsed 2010 tunnel is to the left of the entrance. Photo: Glacier Archaeology Program/Oppland County Council (upper) and L. M. Andreassen (lower).

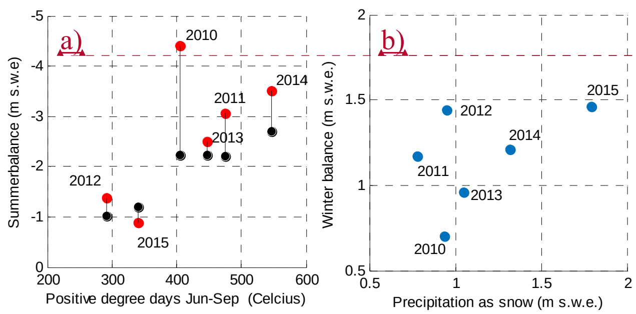

Figure 7. Summer (a~~left~~) and winter (b~~right~~) balance plotted against summer temperature (positive ~~degree days~~degree-days) and precipitation as snow, respectively. For the summer ~~balance~~balance, the black markers are calculated melt using a degree-day model with typical values calibrated from nearby glaciers (3.5 mm/°Cday for snow and 7.5 mm/°Cday for ice). Winter precipitation is obtained from seNorge (Engeset et al., 2004).

Formatted: Font: 14 pt

Formatted: Font: 14 pt, Font color: Auto

Formatted: Font: 14 pt

Formatted: Font: 14 pt, Font color: Auto

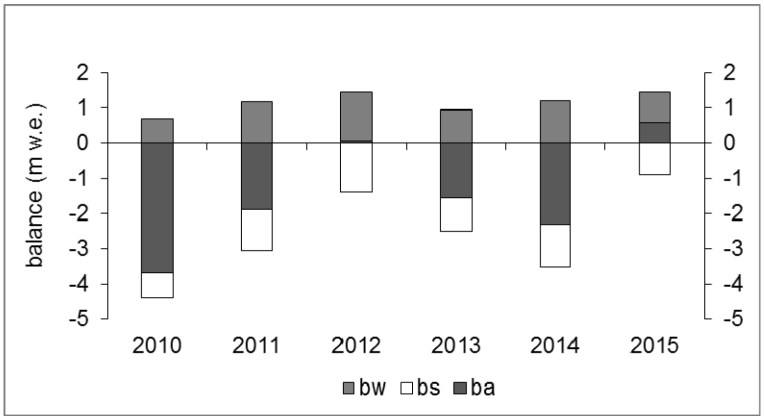

Figure 8. Mass balance measurements at stake J2 on Juvfonne: bw – balance winter, bs – balance summer, ba – annual (net) balance (~~. See figure~~ Fig. 3a for position of stake).

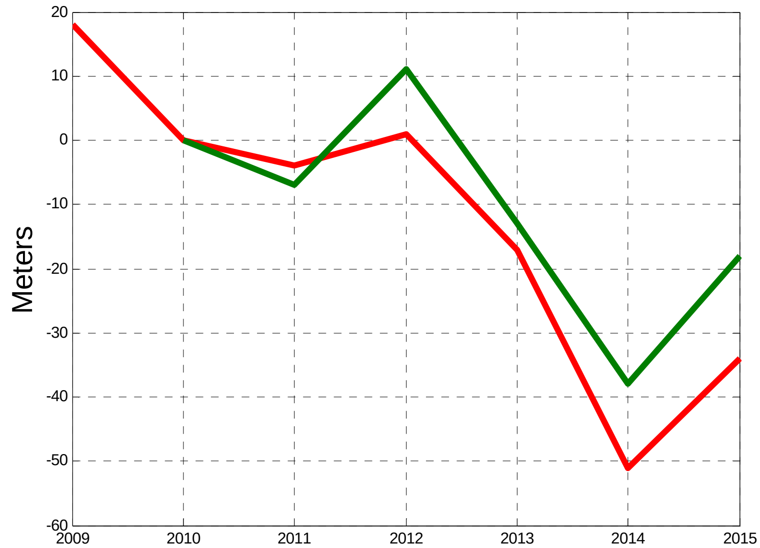

Figure 9. Front position of Juvfonne measured at two locations relative to the 2010-front. Minima are observed in 2011 and 2014. The front retreat 2009-2014 was measured to 69 m. For position of measurements, see ~~figure~~ Fig. 3a. Red - JF1, Green – JF2.

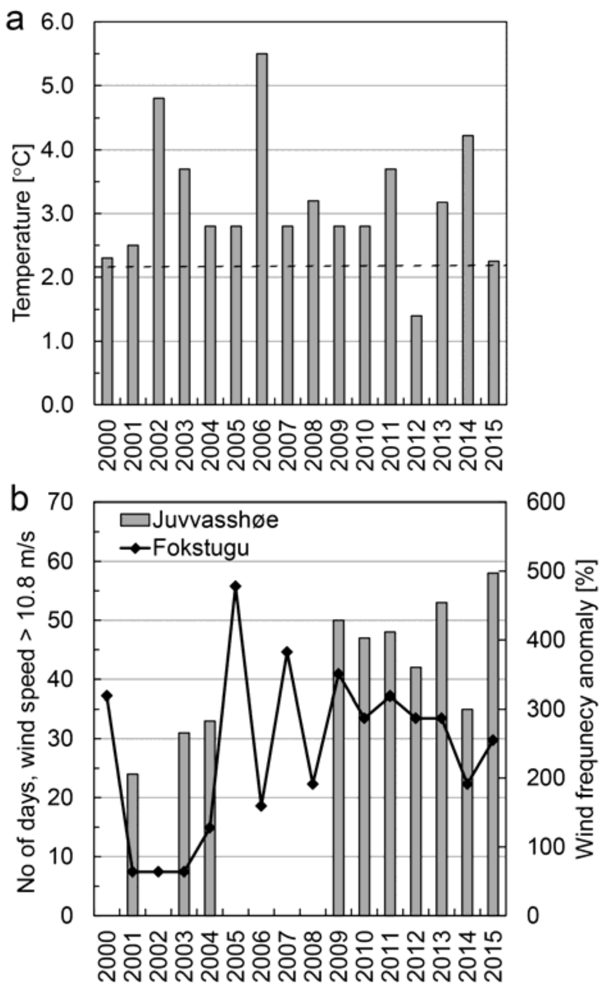

Figure 10. Meteorological data from the station at Juvvasshøe (750 m from the front of Juvfonne) and Fokstugu 70 km NE a) Juvvasshøe June-September mean Air Temperature. The black dotted line denotes the 1971-2000 mean, obtained from the interpolated seNorge dataset (Engeset et al. 2004). b) Number of days for the period June-September with strong breeze or higher (wind speed above 10.8 ms-1) at Juvvasshøe (grey bars) and at Fokstugu (black line), the latter shown as anomaly (in %, right axes) with respect to 1971-2000 mean.

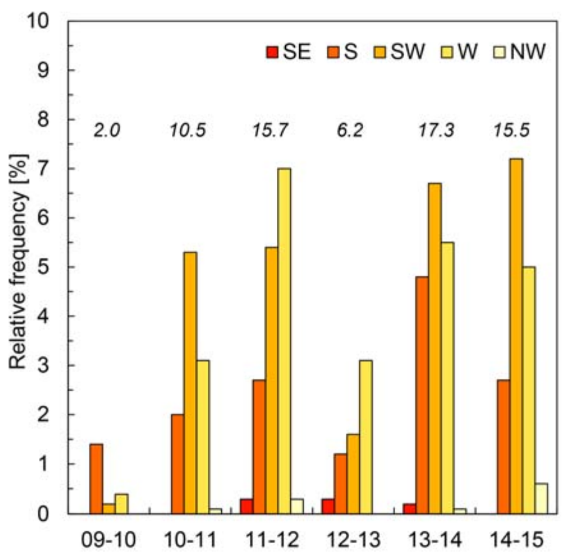

Figure 11. Relative frequency (as percentage of all hourly observations) of strong gale or more (≥ 20.8 ms-1) at Juvvasshøe during winter (Oct-Apr) 2009-2015 for the wind sectors SE to NW. The values inserted show the total frequency of strong gale or more.

Formatted: German (Germany)

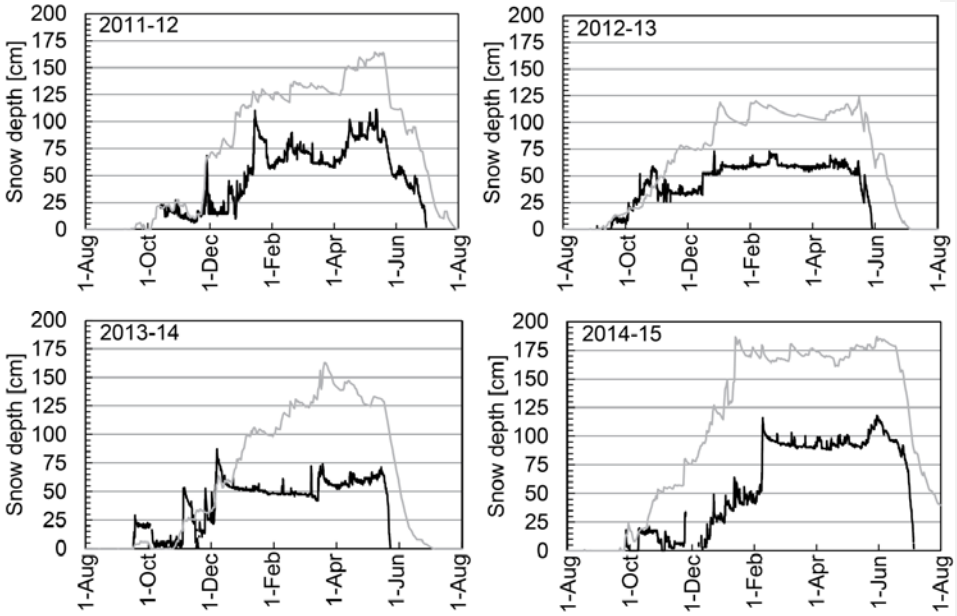

Figure 121. Hourly snow depth measurements (black lines) from the station 95 m from the front of Juvfonne (see Figure 3a for position). Grey lines show modelled daily snow depth from seNorge (Engeset et al. 2004).

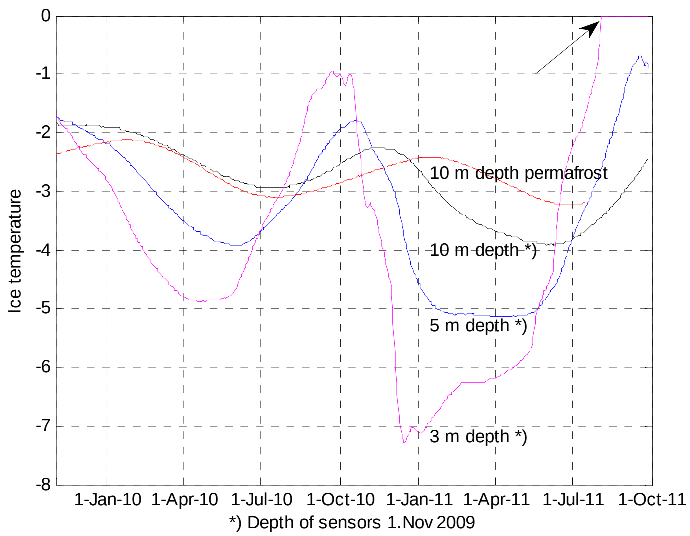
10 m depth permafrost
10 m depth *)
5 m depth *)
3 m depth *)
Ice temperature
1-Jan-10 1-Apr-10 1-Jul-10 1-Oct-10 1-Jan-11 1-Apr-11 1-Jul-11 1-Oct-11
*) Depth of sensors 1.Nov 2009

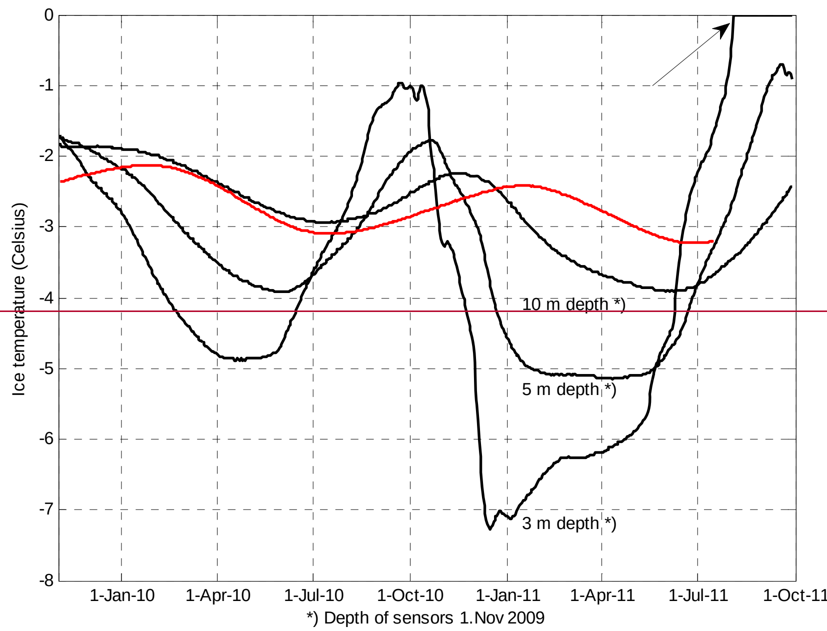
10 m depth *)
5 m depth *)
3 m depth *)
Ice temperature (Celsius)
1-Jan-10 1-Apr-10 1-Jul-10 1-Oct-10 1-Jan-11 1-Apr-11 1-Jul-11 1-Oct-11
*) Depth of sensors 1.Nov 2009

Figure 13~~2~~. Temperature for November 2009-September 2011 in a 10 m deep borehole in the Juvfonne ice patch (see Fig.~~ure~~ 3a for position). The red line is the temperature at 10 m depth in the P31 permafrost borehole 750 m north from the ice patch (see Fig.~~ure~~ 2 for location). Arrow points to the time when the sensor placed at 3 m depth in autumn 2009 melted out. The entire thermistor string melted out in mid-September 2014.

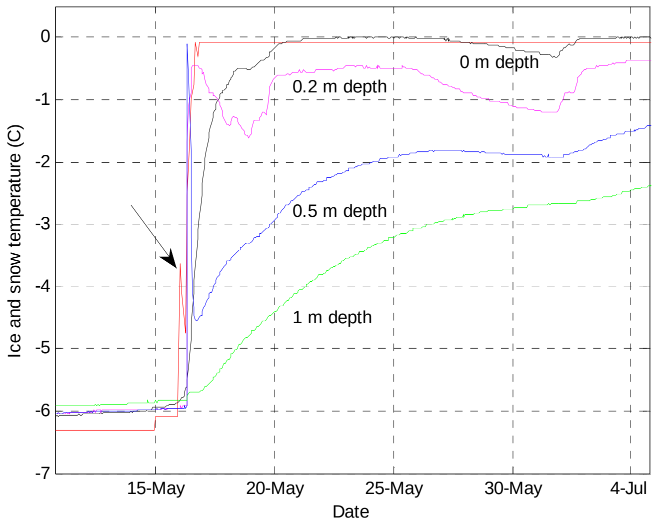
0 m depth
0.2 m depth
0.5 m depth
1 m depth
Ice and snow temperature (C)
0
-1
-2
-3
-4
-5
-6
-7
15-May
20-May
25-May
30-May
4-Jul
Date

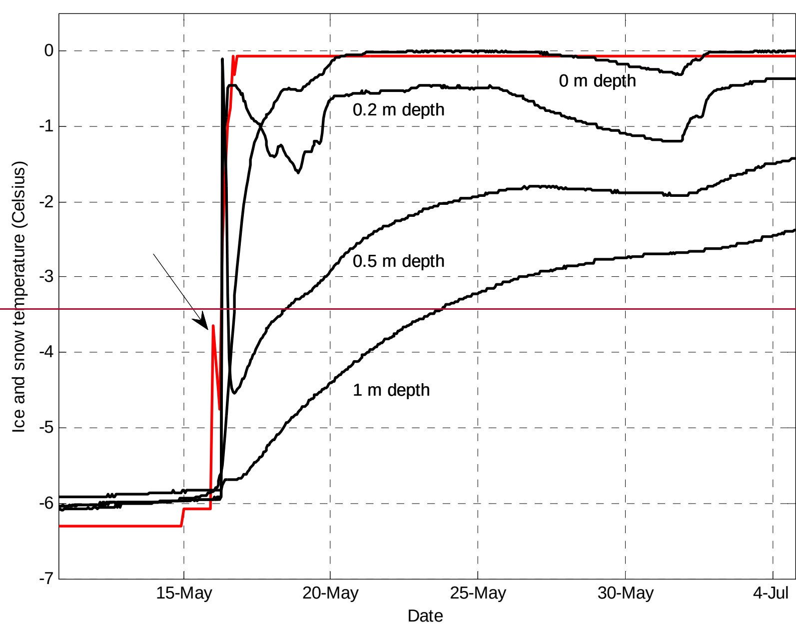
0 m depth
0.2 m depth
0.5 m depth
1 m depth
Ice and snow temperature (Celsius)
0
-1
-2
-3
-4
-5
-6
-7
15-May
20-May
25-May
30-May
4-Jul
Date

Figure 143. Plot of temperature measurements in ice and snow at the onset of thaw in May 2010 (position at the thermistor shown in Fig.figure 3a). The depth reference is the ice surface the previous autumn. The red line is the snow temperature 0.25 m from the base of the snow cover. The arrow point the first signal of surface meltwater refreezing close to the base of the snow cover.

Figure 154. Photo from the old ice tunnel excavated in 2010 showing the layering in the ice and position of two samples for radiocarbon dating. Photo: Klimapark2469 AS.

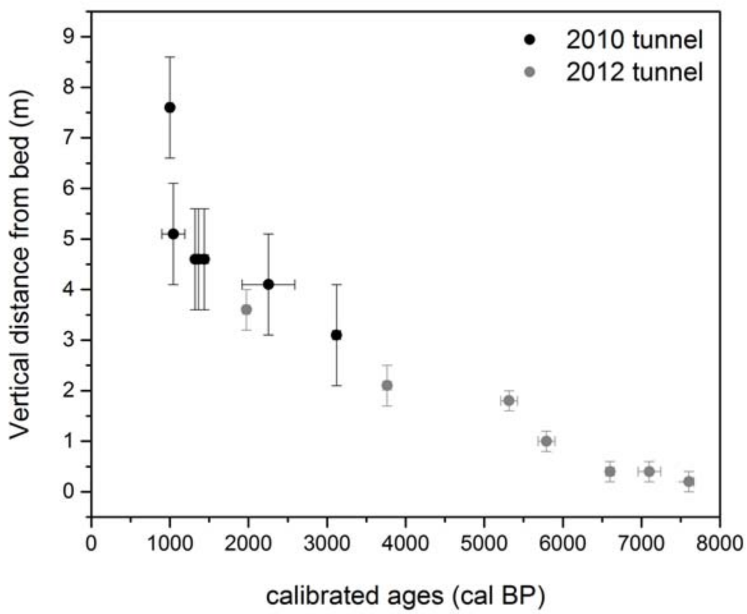

Figure 16. Plot of the samples in Table 2 except samples with modern age. In the inner parts of the 2012 tunnel the bed is partly exposed, which gives good distance to bed estimates. In the 2010 tunnel, the distance estimates depend on the radar data (the old tunnel partly melted out). The horizontal distance between the samples are up to 50 m.

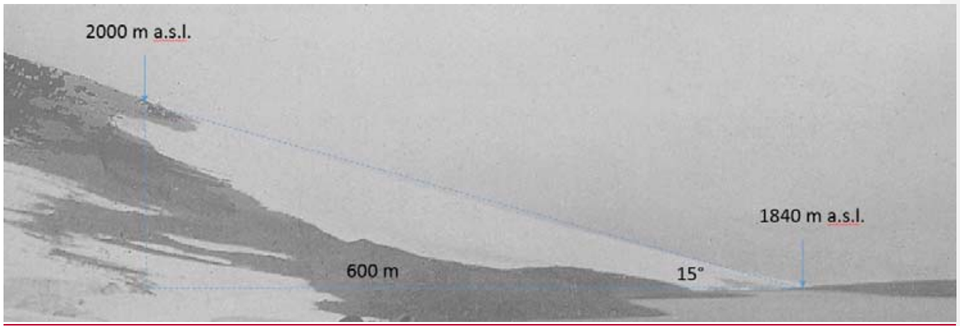

Figure 17. Picture taken from Vesljuvbrea towards NNW, showing Juvfonne from around 1900. The surface slope of Juvfonne is approximately 15°. Height and length estimate from map based on position in the picture. The upper and northern part of Juvfonne cannot be seen on the picture.

Formatted: Line spacing: 1,5 lines, Adjust space between Latin and Asian text, Adjust space between Asian text and numbers

Formatted: Font: (Default) Times New Roman, 12 pt, Font color: Black, English (United Kingdom)

Formatted: Font: (Default) Times New Roman, 12 pt, Font color: Black, English (United Kingdom)

Formatted: Font: (Default) Times New Roman, 12 pt, Font color: Black, English (United Kingdom)